Jacque, J., K. Triques and M. Stevenson, 2002. Modulation of HIV-1 replication by RNA interference. Nature, 26: 1-4.

Joshi, P. and V.R. Prasad, 2002. Potent inhibition of human immunodeficiency virus type 1 replication by template analog reverse transcriptase inhibitors derived by SELEX (systematic evolution of ligands by exponential enrichment). J. Virol., 76: 6545-6557.

Kapadia, S.B., A. Brideau-Andersen and F.V. Chisari, 2003. Interference of hepatitis C virus RNA replication by short interfering RNAs. Proc. Natl. Acad. Sci. USA., 100: 2014-2018.

Kasim, V., M. Miyagishi and K. Taira, 2004. Control of siRNA expression using the Cre-loxP recombination system. Nucleic Acids Res., pp: 32-e66.

Kawasaki, H. and K. Taira, 2002. Identification of genes by hybrid ribozymes that couple cleavage activity with the unwinding activity of an endogenous RNA helicase. EMBO Rep., 3: 443-450.

Khati, M., M. Schuman, J. Ibrahim, Q. Sattentau, S. Gordon and W. James, 2003. Neutralization of infectivity of diverse R5 clinical isolates of human immunodeficiency virus type 1 by gp120-binding 2'F-RNA aptamers. J. Virol., 77: 12692-12698.

Kikuchi, K., T. Umehara, K. Fukuda, A. Kuno, T. Hasegawa and S. Nishikawa, 2005. A Hepatitis C Virus (HCV) Internal Ribosome Entry Site (IRES) domain III-IV-targeted aptamer inhibits translation by binding to an apical loop of domain IIId. Nucleic Acid Res., 33: 683-692.

Lee, N.S., T. Dohjima, G. Bauer, H. Li, M. Li, A. Ehsani, P. Salvaterra and J. Rossi, 2002. Expression of small interfering RNAs targeted against HIV-1 rev transcripts in human cells. Nat. Biotechnol., 19: 500-505.

Lee, T.C., B.A. Sullenger, H.F. Gallardo, G.E. Ungers and E. Gilboa, 1992. Overexpression of RRE-derived sequences inhibits HIV-1 replication in CEM cells. New Biol., 4: 66-74.

Levin, A.A., 1999. A review of issues in the pharmacokinetics and toxicology of phosphorothioate antisense oligonucleotides. Bio. Chem. Biophys. Acta, 1489: 69-84.

Li, H., W.X. Li and S.W. Ding, 2002. Induction and spppression of RNA silencing by an animal virus. Science, 294: 862-864.

Lieber, A., C.Y. He, S.J. Polyak, D.R. Gretch, D. Barr and M.A. Kay, 1996. Elimination of hepatits C virus RNA in infected human hepatocytes by adenovirus-mediated expression of ribozymes. J. Virol., 70: 8782-8791.

Macejak, D.G. K.L. Jensen, S.F. Jamison, K. Domenico, E.C. Roberts, N. Chaudhary, I. von Carlowitz, L. Bellon, M.J. Tong, A. Conrad, P.A. Paveo and L.M. Blatt, 2000. Inhibition of Hepatitis C Virus (HCV)-RNA-dependent translation and replication of a chimeric HCV poliovirus using synthetic stabilized ribozymes. Hepatology, 31: 769-776.

Medina, M.F. and S. Joshi, 1999. Design, characterization and testing of tRNA3Lys-based hammerhead ribozymes. Nucleic Acids Res., 27: 1698-1708.

Michienzi, A., D. Castanotto, N. Lee, S. Li, J.A. Zaia and J.J. Rossi, 2003. RNA-mediated inhibition of HIV in a gene therapy setting. Ann. N.Y. Acad. Sci., 1002: 63-71.

Nishikawa, F., N. Kakiuchi, K. Funaji, K. Fukuda, S. Sekiya and S. Nishikawa, 2003. Inhibition of HCV NS3 protease by RNA aptamers in cells. Nucleic Acids Res., 31: 1935-1943.

Novina, C.D., M.F. Murray, D.M. Dykxhoorn, P.J. Beresford, J. Riess, S.K. Lee, R.G. Collman, J. Lieberman, P. Shankar and P.A. Sharp, 2002. siRNA-directed inhibition of HIV-1 infection. Nat. Med., 8: 681-686.

Ojwang, J.O., A. Hampel, D.J. Looney, F. Wong-Staal and J. Rappaport, 1992. Inhibition of the human immunodeficiency virus type 1 expression by a hairpin ribozyme. Proc. Natl. Acad. Sci. USA., 89: 10802-10806.

Paolella, G., B.S. Sproat and A.I. Lamond, 1992. Nuclease resistant ribozymes with high catalytic activity. EMBO J., 11: 1913-1919.

Peracchi, A., 2004. Prospects for antiviral ribozymes and deoxyribozymes. Rev. Med. Virol., 14: 47-64.

Pieken, W.A., D.B. Olsen, F. Benseler, H. Aurup, and F. Eckstein, 1991. Kinetic characterization of ribonuclease-resistant 2-modified hammerhead ribozymes. Science, 253: 314-317.

Qin, X.F., D.S. An, I.S.Y. Chen and D. Baltimore, 2003. Inhibiting HIV-1 infection in human T cells by lentiviral-mediated delivery of small interfering RNA against CCR5. Proc. Natl. Acad. Sci. USA., 100: 183-188.

Randall, G., A. Grakoui and C.M. Rice, 2003. Clearance of replicating hepatitis C virus replicon RNAs in cell culture by small interfering RNAs. Proc. Natl. Acad. Sci. USA., 100: 235-2340.

Ray, P.S. and S. Das, 2004. Inhibition of hepatitis C virus IRES-mediated translation by small RNAs analogous to stem-loop structures of the 5'-untranslated region. Nucleic Acids Res., 32: 1678-1687.

Schubert, S. H.P. Grunert, H. Zeichhardt, D. Werk, V.A. Erdmann and J. Kurreck, 2005. Maintaining inhibition: siRNA double expression vectors against coxsackieviral RNAs. J. Mol. Biol., 346: 457-465.

Shimayama, T., F. Nishikawa, S. Nishikawa and K. Taira, 1993. Nuclease-resistant chimeric ribozymes containing deoxyribonucleotides and phosphorothicate linkages. Nucleic Acids Res., 21: 2605-2611.

Sullenger, B.A. H.F. Gallardo, G.E. Ungers and E. Gilboa, 1990. Overexpressio.n of TAR sequences renders cells resistant to Human Immunodeficiency Virus replication. Cell, 63: 601-608.

Sullenger, B.A. and T.R. Cech, 1993. Tethering ribozymes to a retroviral packaging signal for destruction of viral RNA. Science, 262: 1566-1569.

Surabhi, R.M. and R.B. Gaynor, 2002. RNA interference directed against viral and cellular targets inhibits human immunodeficiency virus type 1 replication. J. Virol., 76: 12963-12973.

Tuerk, C. and L. Gold, 1990. Systemic evolution of ligands by exponential enrichment: RNA ligands to bacteriophage T4 DNA polymerase. Science, 249: 505-510.

Van de Wetering, M., I. Oving, V. Muncan, M.T. Pon Fong, H. Brantjes, D. Van Leenen, F.C. Holstege, T.R. Brummelkamp, R. Agami and H. Clevers, 2003. Specific inhibition of gene expression using stably integrated, inducible small-interfering-RNA vector. EMBO Rep., 4: 609-615.

Vo, N.V., J.W. Oh, and M.M. Lai, 2003. Identification of RNA ligands that bind hepatitis C virus polymerase selectively and inhibit its RNA synthesis from the natural viral RNA templates. Virology, 307: 301-316.

Welch, P.J., S. Yei and J.R. Barber, 1998. Ribozyme gene therapy for hepatitis C virus infection. Clin. Diagn. Virol., 10: 163-171.

Westerhout, E.M., M. Ooms, M. Vink, A.T. Das and B. Berkhout, 2005. HIV-1 can escape from RNA interference by evolving an alternative structure in its RNA genome. Nucleic Acids Res., 33: 796-804.

Wilson, J.A., S. Jayasena, A. Khvorova, S. Sabatinos, I.G. Rodrigue-Gervais, S. Arya, F. Sarangi, M. Harris-Brandts, S. Beaulieu and C.D. Richardson, 2003. RNA interference blocks gene expression and RNA synthesis from hepatitis C replicons propagated in human liver cells. Proc. Natl. Acad. Sci. USA., 100: 2783-2788.

Yamada, O., G. Kraus, M.C. Leavitt, M. Yu and F. Wong-Staal, 1994. Activity and cleavage site specificity of an anti-HIV hairpin ribozyme in human T cells. Virology, 205: 121-126.

Yamamoto, R., M. Katahira, S. Nishikawa, T. Baba, K. Taira and P.K. Kumar, 2000. A novel RNA motif that binds efficiently and specifically to the Ttat protein of HIV and inhibits the trans-activation by Tat of transcription *in vitro* and *in vivo*. Gene Cells, 5: 371-388.

Yi, R., Y. Qin, I.G. Macara and B.R. Cullen, 2003. Exportin-5 mediates the nuclear export of pre-microRNAs and short hairpin RNAs. Genes Dev., 17: 3011-3016.

Yokota, T. N. Sakamoto, N. Enomoto, Y. Tanabe, M. Miyagishi, S. Maekawa, L. Yi, M. Kurosaki, K. Taira, M. Watanabe and H. Mizusawa, 2003. Inhibition of intracellular hepatitis C virus replication by synthetic and vector-derived small interfering RNAs. EMBO Rep., 4: 602-608.

Zamecnik, P.C. and M.L. Stephenson, 1978. Inhibition of Rous sarcoma virus replication and cell transformation by a specific oligodeoxynucleotide. Proc. Natl. Acad. Sci. USA., 75: 280-284.

Zhang, J., O. Yamada, T. Sakamoto, H. Yoshida, T. Iwai, Y. Matsushita, H. Shimamura, H. Araki and K. Shimotohno, 2004. Down-regulation of viral replication by adenoviral-mediated expression of siRNA against cellular cofactors for hepatitis C virus. Virology, 320: 135-143.

Zhang, J.; O. Yamada, T. Sakamoto, H. Yoshida, H. Araki, T. Murata and K. Shimotohno, 2005. Inhibition of hepatitis C virus replication by pol III-directed overexpression of RNA decoys corresponding to stem-loop structures in the NS5B coding region. Virology, 342: 276-185.

Zhou, C., I.C. Bahner, G.P. Larson, J.A. Zaia, J.J. Rossi and E.B. Kohn, 1994. Inhibition of HIV-1 in human T-lymphocytes by retrovirally transduced anti-tat and rev hammerhead ribozymes. Gene, 149: 33-39.

JOURNAL OF VIROLOGY, Aug. 2007, p. 8722–8729 Vol. 81, No. 16
0022-538X/07/$08.00+0 doi:10.1128/JVI.00253-07

Clathrin-Dependent Entry of Severe Acute Respiratory Syndrome Coronavirus into Target Cells Expressing ACE2 with the Cytoplasmic Tail Deleted▽

Yuuki Inoue,[1] Nobuyuki Tanaka,[1,4]* Yoshinori Tanaka,[1] Shingo Inoue,[3] Kouichi Morita,[3] Min Zhuang,[2] Toshio Hattori,[2] and Kazuo Sugamura[1]

Department of Microbiology and Immunology[1] and Department of Infectious and Respiratory Diseases,[2] Internal Medicine, Tohoku University Graduate School of Medicine, Sendai 980-8575, Japan; Department of Virology, Institute of Tropical Medicine, Nagasaki University, Nagasaki 852-8523, Japan[3]; and Division of Immunology, Miyagi Cancer Center Research Institute, Natori 981-1293, Japan[4]

Received 6 February 2007/Accepted 7 March 2007

The penetration of various viruses into host cells is accomplished by hijacking the host endocytosis machinery. In the case of severe acute respiratory syndrome coronavirus (SARS-CoV) infection, viral entry is reported to require a low pH in intracytoplasmic vesicles; however, little is known about how SARS-CoV invades such compartments. Here we demonstrate that SARS-CoV mainly utilizes the clathrin-mediated endocytosis pathway for its entry to target cells by using infectious SARS-CoV, as well as a SARS-CoV pseudovirus packaged in the SARS-CoV envelope. The SARS-CoV entered caveolin-1-negative HepG2 cells, and the entry was significantly inhibited by treatment with chlorpromazine, an inhibitor for clathrin-dependent endocytosis, and by small interfering RNA-mediated gene silencing for the clathrin heavy chain. Furthermore, the SARS-CoV entered COS7 cells transfected with the mutant of ACE2 with the cytoplasmic tail deleted, SARS-CoV receptor, as well as the wild-type ACE2, and their entries were significantly inhibited by treatment with chlorpromazine. In addition, ACE2 translocated into EEA1-positive early endosomes immediately after the virus attachment to ACE2. These results suggest that when SARS-CoV binds ACE2 it is internalized and penetrates early endosomes in a clathrin-dependent manner and that the cytoplasmic tail of ACE2 is not required for the penetration of SARS-CoV.

Severe acute respiratory syndrome (SARS) is an emerging infectious disease with high mortality caused by infection of the respiratory system by SARS coronavirus (SARS-CoV). SARS-CoV is a human enveloped coronavirus containing a helical nucleocapsid structure composed of a single-stranded, positive-polarity RNA of approximately 29 kb plus the poly(A) tail (44). Phylogenetic analysis classifies the coronaviruses into three groups based on their genetic and serological relationships.

The first essential step in virus infection is the entry of viruses into host cells. After their attachment to their respective cell surface receptor, most viruses make use of cellular endocytosis machineries, such as clathrin-dependent and -independent pathways, for their entry (22, 29). Clathrin-dependent endocytosis has been well characterized using growth factor receptors such as the transferrin receptor (23), epidermal growth factor receptor (EGFR) (39), and the keratinocyte growth factor receptor (3). The endocytosed receptors are translocated into endosomes, where they are degraded or recycled to the cell surface. Similarly, various viruses, among them Semliki Forest virus, vesicular stomatitis virus (VSV), and influenza virus, enter into host cells via the clathrin-dependent endocytosis pathway and translocate into endosomes, where they are uncoated (10, 35, 40). The clathrin-dependent endocytosis is initiated by the binding of adaptor protein 2 (AP2) complexes to the cytoplasmic tail of the cell-surface receptors, which recruits clathrins (27, 38). Subsequently, the receptors are invaginated to form "pits," which are surrounded by a spherical cage-like structure made of clathrin triskelions. Viruses bound to the receptors are endocytosed similarly and then transported to vesicles called early endosomes. It is well known that early endosomes are somewhat acidic (pH 6.5 to 6.0) and become more acidic as they mature to form late endosomes (pH 6.0 to 5.5). The acidification of endosomes is required for incorporated viruses to establish an infection (22, 29).

On the other hand, the clathrin-independent pathways include a caveola-dependent pathway. Caveolae are relatively smaller vesicles of 50 to 100 nm in diameter, formed by membrane invagination at the cell surface, and coated by caveolin-1 (12, 15, 28). Simian virus 40 (SV40), for example, utilizes caveolae to be internalized into the "caveosomes" under a neutral condition (30). In contrast, effective internalization of SV40 was also found in cells that do not express caveolin-1, suggesting that SV40 utilizes not only the caveola-dependent pathway but also the lipid-raft-dependent and caveola-independent pathway (6). Other viruses utilizing the caveola-dependent pathway include some of the picornaviruses (21), papillomaviruses (4), filoviruses (8), and retroviruses (2).

The binding and subsequent entry of SARS-CoV into the host cells are primarily mediated by a viral spike glycoprotein, called S protein, which binds to its receptor, angiotensin-converting enzyme 2 (ACE2) (16). ACE2 is a cell-surface-bound enzyme of the type I membrane protein topology, with its

* Corresponding author. Mailing address: Department of Microbiology and Immunology, Tohoku University Graduate School of Medicine, 2-1 Seiryo-machi, Sendai, 980-8575 Japan. Phone: 81-22-717-8096. Fax: 81-22-717-8097. E-mail: n-tanaka@mail.tains.tohoku.ac.jp.

▽ Published ahead of print on 23 May 2007.

catalytic site exposed to the extracellular surface. ACE2 along with its related family protein ACE is indispensable for blood pressure homeostasis via the renin-angiotensin system (31). However, despite the 40% amino acid identity shared by ACE and ACE2, ACE does not act as a SARS-CoV receptor (25). The broad expression profile of ACE2, which includes the gastrointestinal tract and lungs, matches well with the affected organs in patients with SARS (9). Although accumulating evidence has documented a physical and functional interaction between SARS-CoV and ACE2, little is known about how the ACE2-mediated entry of SARS-CoV is linked to cellular endocytosis machineries.

In the present study, we investigated the internalization mechanisms of SARS-CoV after binding to ACE2. We found that SARS-CoV hijacks the clathrin-dependent machinery for endocytosis via ACE2 with the cytoplasmic tail deleted, as well as the wild-type ACE2.

MATERIALS AND METHODS

Cell lines. The cell lines used here were human hepatoma HepG2 and monkey kidney COS7 cell lines, which were maintained in Dulbecco modified Eagle medium supplemented with 10% fetal calf serum (FCS) and antibiotics, under 5% CO_2 in a humidified incubator.

Virus and infection. SARS-CoV (Vietnam/NB-04/2003) was maintained in Vero E6 cell cultures as described previously (43). In brief, the SARS-CoV titer of the stock virus was determined by infection of Vero E6 cells by a 50% tissue culture infective dose. Cells were inoculated by SARS-CoV at a multiplicity of infection of 1 and allowed to adsorb the virus for 1 h at 4°C. Subsequently, the cells were washed with phosphate-buffered saline (PBS) and cultured for the indicated times. All experiments using infectious SARS-CoV was done in a laboratory certified with biosafety level 3.

RNA extraction and RT-PCR. Total RNA from HepG2 cells infected with SARS-CoV was extracted with the TRIzol reagent (Invitrogen Corp.) by the following the protocol. Reverse transcription-PCR (RT-PCR) for the detection of viral RNA was performed with Titan One-Tube RT-PCR kit (Roche Molecular Systems) by following the manufacturer's protocol. The primer sequences for SARS-CoV detection were gained from World Health Organization network laboratories. The sequence of BNIoutS2 (sense) is 5′-ATGAATTACCAAGTCAATGGTTAC-3′, and the sequence of BNoutAs (antisense) is 5′-CATAACCAGTCGGTACAGCT AC-3′. For an internal control, a primer set of GAPDH (glyceraldehyde-3-phosphate dehydrogenase) was used. The sequence of GAPDH-F (sense) is 5′-AGTC AGCCGCATCTTCTTTTGC-3′, and the sequence of GAPDH-R (antisense) is 5′-CTCCTGGAAGATGGTGATGGGA-3′.

Pseudoviruses. The pseudoviruses were SARS-CoV(HIV), VSV(HIV), and A-MLV (amphotropic murine leukemia virus)(HIV), which consist of the viruses' respective envelope glycoprotein, the HIV Gag/Pol proteins, and a luciferase plasmid. The pseudoviruses were produced with methods described previously (41). In brief, 293T cells were transfected with 7 μg of pCMVΔR8.1 (HIV Gag/Pol plasmid) and 7 μg of pHR′-luciferase, along with an expression vector for the respective viral envelope glycoprotein: 800 ng of pCMV-SARS-S (SARS-CoV S plasmid), 7 μg of pMD.G (VSV G plasmid), or 7 μg of pDJ (A-MLV envelope glycoprotein plasmid). The 293T cells were cultured in 10-cm dishes, and transfection was performed by the calcium phosphate method. At 48 h posttransfection, the culture supernatants were harvested and filtered through 0.45-μm-pore-size screens. These filtered supernatants were used to infect host cells with the pseudoviruses.

Preparation of ACE2 mutants. Three mutants of ACE2 were prepared from pcDNA ACE2 expression vector (20). ACE2-Δtail mutant has a stop codon at the end of the transmembrane domain, ACE2-Δtail-TM mutant is ACE2-Δtail mutant replaced with the transmembrane domain derived from EGFR, and ACE2-sol consists of the extracellular domain of ACE2. The extracellular domains of ACE2-sol from pcDNA ACE2 were amplified by PCR and introduced into pCXN2 after XhoI digestion. These plasmids were transfected with FuGeneHD according to the manufacturer's instructions (Roche Molecular Systems).

Luciferase assay. Cells were infected with pseudovirus for 12 h, and the culture medium was then replaced with virus-free Dulbecco modified Eagle medium. After further 48 h of incubation, the cells were lysed for luciferase assays. The Dual-Luciferase Reporter Assay System (Promega) was used according to the manufacturer's protocol. The luciferase activities of the samples were measured with a Lumat LB 9507 (Berthold).

Inhibition of endocytosis and endosomal acidification. Extraction of cholesterol from the plasma membranes was performed by using methyl-β-cyclodextrin (MBCD; Sigma), as described elsewhere (7). HepG2 cells seeded in a 24- or a 96-well plate 1 day prior to the experiments were treated with serially diluted MBCD for 30 min. After extensive washes with ice-cold PBS, pseudoviruses were added in the absence of MBCD for an additional 12 h. For the inhibition of clathrin-mediated endocytosis, cells were incubated with the respective doses of chlorpromazine (Sigma) for 1 h and then infected with the pseudovirus for an additional 12 h in the presence of chlorpromazine. After extensive washes with PBS, cells were further incubated in the absence of chlorpromazine for 48 h. To determine the pH dependency of the pseudoviruses, the cells were pretreated with serial dilutions of an endosome acidification inhibitor, either NH_4Cl (Sigma) for 1 h, and then infected with pseudoviruses in the presence of the inhibitor. Luciferase activities were determined for cell extracts prepared from these cultures 48 h after the infection.

Immunoblotting. Immunoblotting assays were performed as described previously (17). In brief, cells were lysed in NP-40 lysis buffer (1% Nonidet P-40, 40 mM Tris-HCl [pH 7.5], 150 mM NaCl, 2 mM EDTA, 1 mM phenylmethylsulfonyl fluoride, and 20 μg of aprotinin/ml). The cell lysates were precleared of cellular debris by centrifugation (10,000 × g) for 30 min at 4°C and subjected to sodium dodecyl sulfate-polyacrylamide gel electrophoresis, and the proteins were electrotransferred onto polyvinylidene difluoride membranes (Millipore). The membranes were first blocked with 5% nonfat milk in Tris-buffered saline containing 0.1% Tween 20 and then probed with the indicated primary antibodies. The antibodies used were anti-human CHC (Santa Cruz), anti-α-tubulin (Sigma), and anti-ACE2 (R&D Systems). After three washes, the membranes were probed with horseradish peroxidase-conjugated secondary antibodies (Cell Signaling Technology). Signals were visualized with a Super Signal Pico Detection kit (Pierce), and digital images were collected with a Lumi-Imager F1 (Roche Molecular Systems).

Depletion of CHC by siRNA. To transfect small interfering RNA (siRNA) designed to target the clathrin heavy-chain gene (Invitrogen Corp.), a reverse transfection method was used by using Lipofectamine RNAiMAX (Invitrogen Corp.) according to the manufacturer's instructions. In brief, 5 pmol of stealth siRNA duplex-Lipofectamine RNAiMAX complexes were used for 10^5 HepG2 cells in a 24-well plate. Gene silencing efficiency was assessed 48 h after the transfection by immunoblotting. The siRNA (clathrin heavy chain [CHC]) target sequence was 5′-UGAAGUAUUGACAUCAAAUUUCCGG-3′. A nonfunctional oligonucleotide was used for the control (Invitrogen Corp.).

Immunofluorescence staining. HepG2 cells were grown in 35-mm glass-bottom dishes (Iwaki) at a density of 4×10^4 cells/dish. After 24 h, the cells were washed twice with PBS, fixed with 4% paraformaldehyde for 15 min, washed with the wash buffer (0.1% Triton X-100–PBS), and blocked with the same buffer containing 10% FCS. For immunostaining, samples were incubated overnight with the primary antibodies, including anti-ACE2 and anti-EEA1 (Santa Cruz). After three washes, the samples were incubated with the secondary antibodies (Molecular Probes; Alexa 488-labeled and Alexa 594-labeled antibodies) for 1 h. Confocal imaging was performed by using the 510 META microscope with a 60×/1.30-0.60 oil immersion objective lens (Carl Zeiss).

RESULTS

Effects of endocytosis inhibitors on SARS-CoV entry. To investigate the entry mechanism of SARS-CoV, we used SARS-CoV(HIV), because it allows safe, rapid, and quantitative analyses. Two other pseudoviruses, the VSV(HIV) and A-MLV(HIV), were used as control viruses, because VSV(HIV) utilizes the pH-dependent and clathrin-dependent entry mechanisms (40), while A-MLV(HIV) utilizes the pH-independent and clathrin-independent entry mechanisms (2, 25, 40).

HepG2 cells were infected with pseudoviruses, SARS-CoV-(HIV), VSV(HIV), or A-MLV(HIV) in the presence of an endocytosis inhibitor, chlorpromazine. Chlorpromazine is a cationic amphiphilic drug that disrupts clathrin-mediated endocytosis by inhibiting the relocation of clathrin and AP2 from the cell surface (42). HepG2 cells were pretreated with various

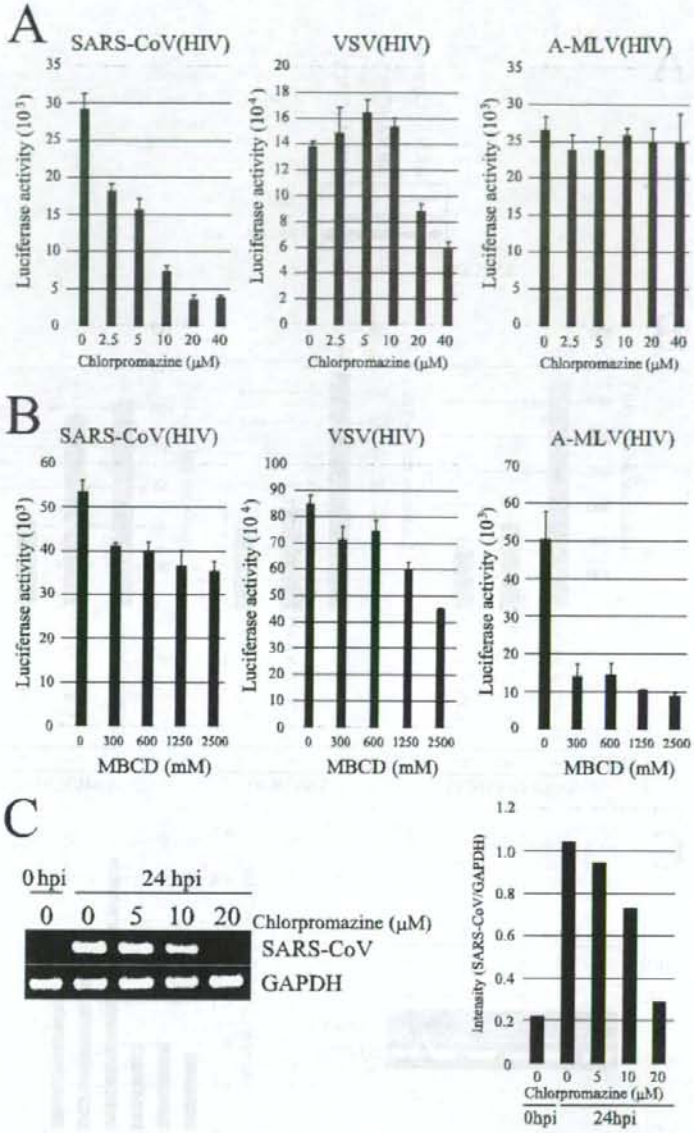

FIG. 1. Effects of chlorpromazine and MBCD on pseudoviruses and SARS-CoV infection. (A and B) HepG2 cells were treated with the indicated doses of chlorpromazine or MBCD and then infected with SARS-CoV(HIV), VSV(HIV), or A-MLV(HIV) for overnight. The effects of chlorpromazine and MBCD on the infectivity of each pseudovirus were evaluated by measuring the luciferase activities. The columns represent the mean values of triplicate experiments; bars indicate maximum values. (C) HepG2 cells treated with the indicated doses of chlorpromazine were infected with SARS-CoV (Vietnam/NB-04/2003) for 24 h, and their expressions of viral RNA were measured by RT-PCR.

doses of chlorpromazine for 1 h and then infected with the indicated pseudovirus in the presence of chlorpromazine (Fig. 1A). Chlorpromazine significantly inhibited the infection efficiency of SARS-CoV(HIV); only 14% infectivity was observed with 20 μM chlorpromazine. Infection by VSV(HIV) was also inhibited, but less so; 42% infectivity was still seen with 20 μM chlorpromazine. Unlike the other two pseudoviruses, infection by A-MLV(HIV) was largely unaffected by any concentration of chlorpromazine.

We also examined the effects of another endocytosis inhibitor, MBCD, on infections by the pseudoviruses, because MBCD disrupts cholesterol-rich microdomains, resulting in

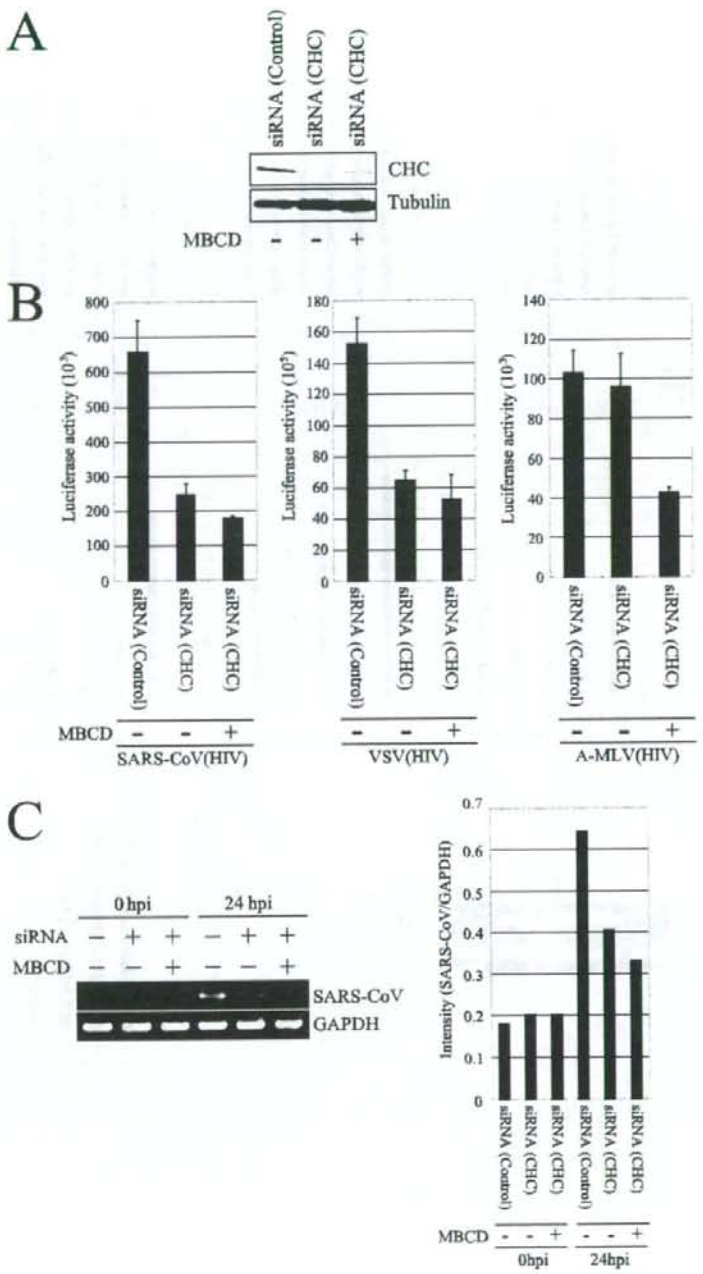

FIG. 2. Effects of CHC-specific siRNA on pseudoviruses and SARS-CoV infection. (A) HepG2 cells were transfected with the CHC-specific siRNA or the control siRNA and analyzed by immunoblotting with anti-CHC or anti-tubulin monoclonal antibody after 48 h of transfection. (B) The cells were treated with 2.5 mM MBCD for 30 min and then infected with each pseudovirus. The infectivities of the pseudoviruses are represented as luciferase activities. The experiment was performed in triplicate. (C) The cells were also infected with SARS-CoV (Vietnam/NB-04/2003) for 24 h, and their expressions of viral RNA were measured by RT-PCR.

the inhibition of both the caveola-dependent endocytosis and caveola-independent lipid-raft-dependent endocytosis (18, 32). HepG2 cells were treated with various concentrations of MBCD for 30 min and thereafter infected with the pseudoviruses in the absence of MBCD to avoid any potential effect of MBCD on the viral envelopes (Fig. 1B). MBCD treatment inhibited the susceptibility of HepG2 cells to A-MLV(HIV), to 18% of the control level at 2500 μM MBCD, whereas only a modest reduction in the cells' susceptibility to the SARS-CoV-(HIV) and VSV(HIV) was seen, to 66 and 53% of the control, respectively (Fig. 1B).

We next used SARS-CoV (Vietnam/NB-04/2003). HepG2 cells were treated or untreated with indicated concentrations of chlorpromazine for 1 h and then infected with SARS-CoV for 24 h. Infection efficiency of SARS-CoV was determined by RT-PCR. It was significantly inhibited by chlorpromazine treatment (Fig. 1C). Collectively, these results suggest that SARS-CoV entry into HepG2 cells is mostly mediated by the clathrin-dependent pathway, although some SARS-CoV pseudovirus entry appears to be dependent on caveolae and/or lipid rafts.

Effect of CHC depletion on SARS-CoV entry. To examine whether clathrin-mediated endocytosis is required for SARS-CoV(HIV) entry, we used siRNA-mediated gene silencing against the major component of the clathrin triskelion, CHC. In addition, under this clathrin knockdown condition, we simultaneously inhibited the clathrin-independent pathways with MBCD. This method was designed to determine whether the pseudoviruses entered the cells via the clathrin-dependent or -independent pathways, or both.

Transfection of a specific siRNA for CHC reduced the CHC protein expression to less than 10% of that in the control siRNA-transfected HepG2 cells, and we observed no effect of MBCD treatment on the CHC knockdown (Fig. 2A). CHC-depleted MBCD-treated cells, CHC-depleted mock-treated cells, and control cells were infected with the SARS-CoV(HIV), VSV(HIV), and A-MLV(HIV). CHC depletion reduced the SARS-CoV-(HIV) infectivity to 38% and the infectivity of VSV(HIV) to 42% of that in the control cells. Cholesterol depletion by MBCD in the CHC knockdown cells reduced the SARS-CoV(HIV) infectivity to 28% and the infectivity of VSV(HIV) to 36% of their infectivity in the control cells (Fig. 2B). On the other hand, there was little effect on the A-MLV(HIV) infectivity in cells expressing the siRNA. However, MBCD treatment markedly reduced the A-MLV(HIV) infectivity to 41% (Fig. 2B). The *t* test revealed the statistical significances in combinations between MBCD-treated and -untreated CHC knockdown cells infected with the pseudoviruses.

We also examined the effect of clathrin knockdown on SARS-CoV (Vietnam/NB-04/2003) infection to HepG2 cells under a similar condition to the pseudoviruses. CHC depletion reduced the SARS-CoV infectivity to 65% of that in the control cells at 24 h postinfection. Cholesterol depletion by MBCD in the CHC-knockdown cell slightly inhibited to this effect (Fig. 2C). These results support the evidence described above that the clathrin-mediated pathway of endocytosis is required for an efficient SARS-CoV entry into HepG2 cells.

Receptor activities of ACE2 mutants for SARS-CoV infection. To further investigate the clathrin-dependent endocytosis of SARS-CoV, we sought to determine whether the cytoplasmic domain of ACE2 is required for interaction with AP2/clathrin complexes. We prepared an ACE2 mutant (ACE2-Δtail) that lacks the cytoplasmic domain by introduction of the stop codon at the end of the transmembrane domain of ACE2. The virus receptor activity of ACE2 mutant was examined with COS7 cells because COS7 cells are negative for ACE2 expression detected by RT-PCR and immunoblotting but positive for caveolin-1 (data not shown) (34). COS7 cells transfected with ACE2-Δtail were infected with SARS-CoV(HIV) equally well to the cells transfected with the wild-type ACE2 (Fig. 3A and

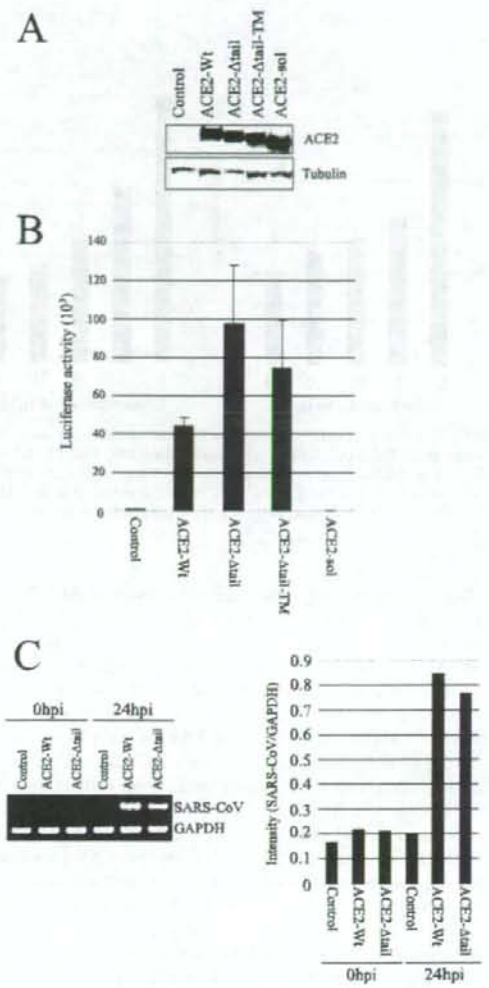

FIG. 3. Receptor activity of ACE2 mutants for pseudoviruses and SARS-CoV infection. (A) COS7 cells were transiently transfected with ACE2-wt, ACE2-Δtail, ACE2-Δtail-TM, ACE2-sol or control plasmids, and after 48 h of transfection their lysates were tested by immunoblotting with anti-ACE2 or anti-tubulin monoclonal antibody. (B and C) The transfected cells were infected with SARS-CoV(HIV) (B) or SARS-CoV (Vietnam/NB-04/2003) (C). Their luciferase activities were measured in triplicate, and their expressions of viral RNA were measured by RT-PCR.

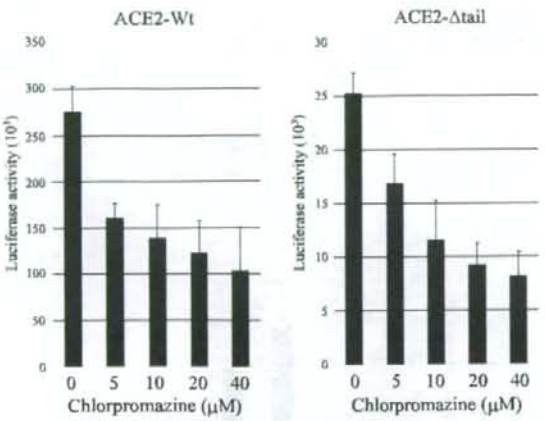

FIG. 4. Effects of chlorpromazine on pseudovirus infection to cells expressing ACE2-Δtail. COS7 cells were transiently transfected with ACE2-wt or ACE2-Δtail and then treated with the indicated amounts of chlorpromazine. Subsequently, the cells were infected with SARS-CoV(HIV). Their luciferase activities were measured in triplicate.

B). We further examined the receptor activity of ACE2-Δtail-TM, which lacks the cytoplasmic domain and replaces the transmembrane domain with that derived from EGFR. ACE2-Δtail-TM also showed a receptor activity for SARS-CoV(HIV) (Fig. 3B). We also confirmed that ACE2-sol, a soluble form of the ACE2 extracellular domain, has no receptor activity for SARS-CoV(HIV). Next, we used SARS-CoV (Vietnam/NB-04/2003). COS7 cells transfected with ACE2-Δtail were also infected with SARS-CoV equally well to the cells transfected with the wild-type ACE2 at 24 h postinfection (Fig. 3C). These results suggest that the cytoplasmic domain of ACE2 is not essential for its receptor activity and that there is no specificity of the transmembrane domain for its receptor activity.

We next confirmed that the ACE2-Δtail-mediated infection of SARS-CoV(HIV) is also clathrin dependent. COS7 cells transfected with the wild-type ACE2 or ACE2-Δtail were pretreated with chlorpromazine and infected with SARS-CoV-(HIV). The chlorpromazine treatment induced suppression of SARS-CoV(HIV) infection to COS7 cells expressing ACE2-Δtail, as well as the wild-type ACE2 (Fig. 4).

SARS-CoV(HIV) is transported into EEA1-positive early endosomes. Accumulating evidence suggests that cell surface molecules internalized by the clathrin-dependent pathway are transferred into early endosomes. We used confocal microscopy to examine whether ACE2 is internalized in early endosomes upon SARS-CoV(HIV) binding. After a 3 h period of serum starvation, HepG2 cells expressed ACE2 predominantly on the cell surface (Fig. 5, upper panels). The cells were then infected with SARS-CoV(HIV) concentrated 10-fold by ultracentrifuge. By 10 min after the infection, the ACE2 localization had changed dramatically, from the cell surface to EEA1-positive early endosomes (Fig. 5, lower panels). We also confirmed that the SARS-CoV(HIV) entry was affected by acidification inhibitors such as ammonium chloride (NH_4Cl) and chloroquine (data not shown). Furthermore, we examined the effect of ammonium chloride on SARS-CoV(HIV) infection into COS7 cells expressing ACE2-

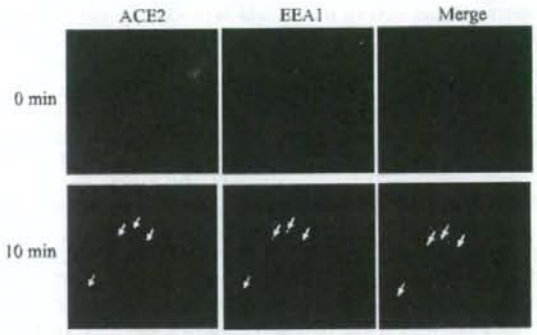

FIG. 5. Immunohistochemical localization of ACE2 after pseudovirus infection. HepG2 cells were cultured in the FCS-free medium to induce ACE2 on cell surfaces and incubated with concentrated SARS-CoV-(HIV) for 10 min at 37°C. They were then stained for ACE2 and EEA1 by immunofluorescence.

Δtail (Fig. 6). The ammonium chloride treatment induced inhibition of SARS-CoV(HIV) infection in a manner similar to that for HepG2 cells. These results suggest that the binding of the SARS-CoV(HIV) to ACE2 induces rapid internalization of the ACE2/pseudovirus complex into EEA1-positive early endosomes, where a low pH condition is required for it to establish an infection and that the cytoplasmic tail of ACE2 is not required for the internalization of SARS-CoV(HIV) into endosomes.

DISCUSSION

Productive infection of target cells by animal viruses requires their access to highly specific entry pathways that allow

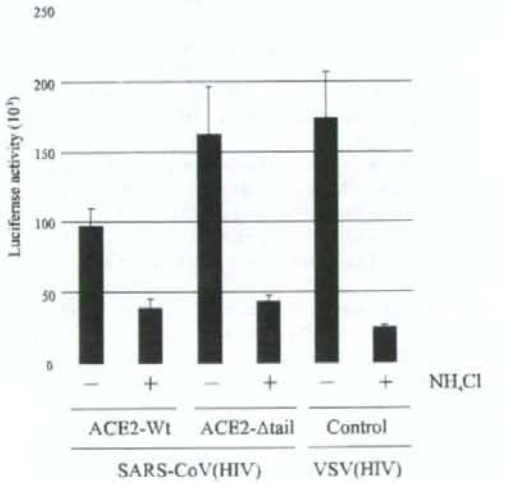

FIG. 6. Dependence on acidic environment for infection by the pseudoviruses. COS7 cells transiently transfected with ACE2-wt, ACE2-Δtail, or control plasmids were treated with 20 mM NH_4Cl and then infected with SARS-CoV(HIV) and VSV(HIV). Their infectivities were evaluated by measuring the luciferase activity. The experiment was performed in triplicate.

critical virion components to be introduced into the cytoplasm for subsequent processes, including uncoating, gene expression, and replication. The present study documented that the main pathway of SARS-CoV entry into host cells is dependent on clathrin. Chlorpromazine is a cationic amphiphilic agent that inhibits the formation of clathrin-coated pits (24). The use of chlorpromazine has established that a number of other viruses, including VSV (40) and influenza virus (36), use clathrin for entry into the host cell. We found that chlorpromazine inhibited the infection of HepG2 cells by SARS-CoV(HIV) more significantly than by VSV(HIV). We also confirmed the inhibitory effect of chlorpromazine on the SARS-CoV (Vietnam/NB-04/2003) infection to HepG2 cells. Moreover, HepG2 cells used here are unable to form caveolae because of no expression of caveolin-1 (data not shown). These results suggest that the SARS-CoV entry is mainly mediated by clathrin-coated pits. The specificity of the chlorpromazine effect was supported by the observation that the chlorpromazine treatment had little effect on the entry of the clathrin-independent A-MLV(HIV). To verify SARS-CoV's dependence on clathrin for host cell entry, we used CHC knockdown HepG2 cells as the target for SARS-CoV infection. The treatment of HepG2 cells with CHC siRNA induced significant suppression of the SARS-CoV(HIV) infection, as well as the SARS-CoV infection. Furthermore, we found that the ACE2 is colocalized with the CHC out of the lipid raft. Hence, although we cannot exclude a minor contribution of the clathrin-independent pathway to SARS-CoV(HIV) entry, the clathrin-dependent pathway is probably the main one used by SARS-CoV for host cell entry.

A previous report demonstrated that an ACE2 mutant partially deleted of the cytoplasmic domain sustains a receptor activity for SARS-CoV infection (11). Since we found that the ACE2-mediated infection of SARS-CoV is mainly clathrin dependent, we then definitively sought to determine whether the cytoplasmic domain of ACE2 is required for the clathrin-dependent pathway of SARS-CoV infection. We prepared an ACE2 mutant, ACE2-Δtail, with the cytoplasmic domain completely deleted, and demonstrated that the SARS-CoV infection via the ACE2-Δtail is mainly clathrin dependent because chlorpromazine inhibits the ACE2-Δtail-mediated entry of SARS-CoV(HIV) into COS7 cells. These results indicate that the cytoplasmic domain of the ACE2 is not essential for the clathrin-dependent entry of SARS-CoV, which suggests that there is a possible coreceptor for the ACE2, which interacts with the AP2/clathrin complex. The replacement of the transmembrane domain of ACE2 with that of EGFR showed no effect on the susceptibility of the cells to SARS-CoV. Since the ACE2 extracellular domain alone is unable to induce the receptor activity, the extracellular domain containing the transmembrane domain is indispensable for the receptor activity for SARS-CoV but the cytoplasmic tail of ACE2 is dispensable.

SARS-CoV infection was previously shown to be suppressed partially by treatment of the cholesterol-depleting reagent, MBCD (19). We also observed lower but significant levels of MBCD-mediated suppression of the SARS-CoV(HIV) and VSV(HIV) infection compared to the A-MLV(HIV) infection. The difference in MBCD's suppressive effects between A-MLV(HIV) and the other two pseudoviruses may be explained by the possibility that the SARS-CoV(HIV) entry might be partially mediated by a clathrin-independent pathway corresponding to the lipid raft-mediated pathway. Alternatively, in a previous report, MBCD partially inhibited the clathrin-mediated endocytosis of transferrin receptor and EGFR, as well as completely inhibiting their lipid raft- and/or caveola-mediated endocytosis (14, 33), suggesting that MBCD might have some unexpected effect on the clathrin-mediated pathway for the SARS-CoV infection. To address these possibilities, we investigated the additive or synergistic effect of MBCD with CHC-siRNA on the SARS-CoV infection to HepG2 cells. MBCD induced a weak but significant additive suppression on CHC-siRNA-treated HepG2 cell infection by SARS-CoV, suggesting a minor clathrin-independent entry pathway for SARS-CoV.

The SARS-CoV S protein is cleaved into S1 and S2 proteins by an acidic protease, cathepsin L, in endosomes, which is essential for fusion between the viral envelope and the endosome vesicular membrane (1, 13, 37). We demonstrated here the translocation of ACE2 to the EEA1-positive endosomes upon SARS-CoV(HIV) infection and showed the suppressive effects of acidification inhibitors, NH_4Cl and chloroquine, on SARS-CoV(HIV) infection to HepG2 cells. Furthermore, the SARS-CoV(HIV) infection to COS7 cells expressing ACE2-Δtail was significantly suppressed by NH_4Cl treatment, suggesting that SARS-CoV infection via ACE2-Δtail is not different from that via the wild-type ACE2.

Based on the present study, we propose a model for SARS-CoV's internalization by target cells. SARS-CoV attaches the cell surface through an interaction between the envelope spike glycoprotein and its receptor, ACE2. Clathrin-coated pits are then formed by interactions between the ACE2/virus complex and the AP2/clathrin complex via a possible coreceptor in a non-lipid-raft portion of the plasma membrane. The ACE2/virus complex is then translocated to endosomes, where the virus is uncoated by the help of endosomal acid protease, such as cathepsin L (13, 37).

Among the *Coronaviridae*, human coronavirus 229E (HCoV-229E) utilizes aminopeptidase N (CD13) as its receptor, which is localized in the lipid rafts, and HCoV-229E infection is inhibited by the treatment of target cells with MBCD and the transfection of an siRNA specific for caveolin-1, suggesting that HCoV-229E utilizes the caveola-mediated endocytosis pathway for its entry into target cells (26). Since CD13 is a common viral receptor for other group 1 coronaviruses, such as porcine transmissible gastroenteritis virus, porcine epidemic diarrhea virus, feline infectious peritonitis virus, and canine coronavirus, the caveola-mediated endocytosis pathway seems to be conserved among them. In contrast, murine hepatitis virus, which is a group 2 coronavirus, was previously shown to utilize the lipid raft-mediated endocytosis pathway (5). Hence, SARS-CoV, which is also classified into the group 2 coronavirus, seems to be unique among the *Coronaviridae* because it utilizes the clathrin-mediated pathway for its entry into HepG2 and COS7 cells.

ACKNOWLEDGMENTS

This study was supported in part by Grants-in-Aid for Scientific Research from the Japan Society for the Promotion of Science, for Scientific Research on Priority Areas, and for a Center of Excellence program of the Ministry of Education, Science, Sports, and Culture of the Japanese Government, and for Research on Emerging and Re-emerging Infectious Diseases of the Ministry of Health, Labor and Welfare.

We thank Lamichanem Aayam for critical reading of the manuscript.

REFERENCES

1. **Ashraf, H.** 2005. Cathepsin enzyme provides clue to SARS infection. Drug Discov. Today **10:**1409.
2. **Beer, C., D. S. Andersen, A. Rojek, and L. Pedersen.** 2005. Caveola-dependent endocytic entry of amphotropic murine leukemia virus. J. Virol. **79:** 10776–10787.
3. **Belleudi, F., V. Visco, M. Ceridono, L. Leone, R. Muraro, L. Frati, and M. R. Torrisi.** 2003. Ligand-induced clathrin-mediated endocytosis of the keratinocyte growth factor receptor occurs independently of either phosphorylation or recruitment of eps15. FEBS Lett. **553:**262–270.
4. **Bousarghin, L., A. Touze, P. Y. Sizaret, and P. Coursaget.** 2003. Human papillomavirus types 16, 31, and 58 use different endocytosis pathways to enter cells. J. Virol. **77:**3846–3850.
5. **Choi, K. S., H. Aizaki, and M. M. Lai.** 2005. Murine coronavirus requires lipid rafts for virus entry and cell-cell fusion but not for virus release. J. Virol. **79:**9862–9871.
6. **Damm, E. M., L. Pelkmans, J. Kartenbeck, A. Mezzacasa, T. Kurzchalia, and A. Helenius.** 2005. Clathrin- and caveolin-1-independent endocytosis: entry of simian virus 40 into cells devoid of caveolae. J. Cell Biol. **168:**477–488.
7. **Danthi, P., and M. Chow.** 2004. Cholesterol removal by methyl-beta-cyclodextrin inhibits poliovirus entry. J. Virol. **78:**33–41.
8. **Empig, C. J., and M. A. Goldsmith.** 2002. Association of the caveola vesicular system with cellular entry by filoviruses. J. Virol. **76:**5266–5270.
9. **Gembardt, F., A. Sterner-Kock, H. Imboden, M. Spalteholz, F. Reibitz, H. P. Schultheiss, W. E. Siems, and T. Walther.** 2005. Organ-specific distribution of ACE2 mRNA and correlating peptidase activity in rodents. Peptides **26:**1270–1277.
10. **Helenius, A., J. Kartenbeck, K. Simons, and E. Fries.** 1980. On the entry of Semliki Forest virus into BHK-21 cells. J. Cell Biol. **84:**404–420.
11. **Hofmann, H., M. Geier, A. Marzi, M. Krumbiegel, M. Peipp, G. H. Fey, T. Gramberg, and S. Pohlmann.** 2004. Susceptibility to SARS coronavirus S protein-driven infection correlates with expression of angiotensin converting enzyme 2 and infection can be blocked by soluble receptor. Biochem. Biophys. Res. Commun. **319:**1216–1221.
12. **Hommelgaard, A. M., K. Roepstorff, F. Vilhardt, M. L. Torgersen, K. Sandvig, and B. van Deurs.** 2005. Caveolae: stable membrane domains with a potential for internalization. Traffic **6:**720–724.
13. **Huang, I. C., B. J. Bosch, F. Li, W. Li, K. H. Lee, S. Ghiran, N. Vasilieva, T. S. Dermody, S. C. Harrison, P. R. Dormitzer, M. Farzan, P. J. Rottier, and H. Choe.** 2006. SARS coronavirus, but not human coronavirus NL63, utilizes cathepsin L to infect ACE2-expressing cells. J. Biol. Chem. **281:**3198–3203.
14. **Imelli, N., O. Meier, K. Boucke, S. Hemmi, and U. F. Greber.** 2004. Cholesterol is required for endocytosis and endosomal escape of adenovirus type 2. J. Virol. **78:**3089–3098.
15. **Insel, P. A., B. P. Head, R. S. Ostrom, H. H. Patel, J. S. Swaney, C. M. Tang, and D. M. Roth.** 2005. Caveolae and lipid rafts: G protein-coupled receptor signaling microdomains in cardiac myocytes. Ann. N. Y. Acad. Sci. **1047:** 166–172.
16. **Kuhn, J. H., W. Li, H. Choe, and M. Farzan.** 2004. Angiotensin-converting enzyme 2: a functional receptor for SARS coronavirus. Cell Mol. Life Sci. **61:**2738–2743.
17. **Kyuuma, M., K. Kikuchi, K. Kojima, Y. Sugawara, M. Sato, N. Mano, J. Goto, T. Takeshita, A. Yamamoto, K. Sugamura, and N. Tanaka.** 2007. AMSH, an ESCRT-III associated enzyme, deubiquitinates cargo on MVB/late endosomes. Cell Struct. Funct. **31:**159–172.
18. **Lambert, S., D. Vind-Kezunovic, S. Karvinen, and R. Gniadecki.** 2006. Ligand-independent activation of the EGFR by lipid raft disruption. J. Investig. Dermatol. **126:**954–962.
19. **Li, G. M., Y. G. Li, M. Yamate, S. M. Li, and K. Ikuta.** 2007. Lipid rafts play an important role in the early stage of severe acute respiratory syndrome-coronavirus life cycle. Microbes Infect. **9:**96–102.
20. **Li, W., M. J. Moore, N. Vasilieva, J. Sui, S. K. Wong, M. A. Berne, M. Somasundaran, J. L. Sullivan, K. Luzuriaga, T. C. Greenough, H. Choe, and M. Farzan.** 2003. Angiotensin-converting enzyme 2 is a functional receptor for the SARS coronavirus. Nature **426:**450–454.
21. **Marjomaki, V., V. Pietiainen, H. Matilainen, P. Upla, J. Ivaska, L. Nissinen, H. Reunanen, P. Huttunen, T. Hyypia, and J. Heino.** 2002. Internalization of echovirus 1 in caveolae. J. Virol. **76:**1856–1865.
22. **Marsh, M., and A. Helenius.** 2006. Virus entry: open sesame. Cell **124:**729–740.
23. **Mellman, I.** 1996. Endocytosis and molecular sorting. Annu. Rev. Cell Dev. Biol. **12:**575–625.
24. **Nawa, M., T. Takasaki, K. Yamada, I. Kurane, and T. Akatsuka.** 2003. Interference in Japanese encephalitis virus infection of Vero cells by a cationic amphiphilic drug, chlorpromazine. J. Gen. Virol. **84:**1737–1741.
25. **Nie, Y., P. Wang, X. Shi, G. Wang, J. Chen, A. Zheng, W. Wang, Z. Wang, X. Qu, M. Luo, L. Tan, X. Song, X. Yin, M. Ding, and H. Deng.** 2004. Highly infectious SARS-CoV pseudotyped virus reveals the cell tropism and its correlation with receptor expression. Biochem. Biophys. Res. Commun. **321:** 994–1000.
26. **Nomura, R., A. Kiyota, E. Suzaki, K. Kataoka, Y. Ohe, K. Miyamoto, T. Senda, and T. Fujimoto.** 2004. Human coronavirus 229E binds to CD13 in rafts and enters the cell through caveolae. J. Virol. **78:**8701–8708.
27. **Pearse, B. M., C. J. Smith, and D. J. Owen.** 2000. Clathrin coat construction in endocytosis. Curr. Opin. Struct. Biol. **10:**220–228.
28. **Pelkmans, L.** 2005. Secrets of caveolae- and lipid raft-mediated endocytosis revealed by mammalian viruses. Biochim. Biophys. Acta **1746:**295–304.
29. **Pelkmans, L., and A. Helenius.** 2003. Insider information: what viruses tell us about endocytosis. Curr. Opin. Cell Biol. **15:**414–422.
30. **Pietiainen, V. M., V. Marjomaki, J. Heino, and T. Hyypia.** 2005. Viral entry, lipid rafts and caveosomes. Ann. Med. **37:**394–403.
31. **Prabakaran, P., X. Xiao, and D. S. Dimitrov.** 2004. A model of the ACE2 structure and function as a SARS-CoV receptor. Biochem. Biophys. Res. Commun. **314:**235–241.
32. **Riemann, D., G. H. Hansen, L. Niels-Christiansen, E. Thorsen, L. Immerdal, A. N. Santos, A. Kehlen, J. Langner, and E. M. Danielsen.** 2001. Caveolae/lipid rafts in fibroblast-like synoviocytes: ectopeptidase-rich membrane microdomains. Biochem. J. **354:**47–55.
33. **Rodal, S. K., G. Skretting, O. Garred, F. Vilhardt, B. van Deurs, and K. Sandvig.** 1999. Extraction of cholesterol with methyl-beta-cyclodextrin perturbs formation of clathrin-coated endocytic vesicles. Mol. Biol. Cell **10:**961–974.
34. **Sha, Y., Y. Wu, Z. Cao, X. Xu, W. Wu, D. Jiang, X. Mao, H. Liu, Y. Zhu, R. Gong, and W. Li.** 2006. A convenient cell fusion assay for the study of SARS-CoV entry and inhibition. IUBMB Life. **58:**480–486.
35. **Sieczkarski, S. B., and G. R. Whittaker.** 2005. Characterization of the host cell entry of filamentous influenza virus. Arch. Virol. **150:**1783–1796.
36. **Sieczkarski, S. B., and G. R. Whittaker.** 2003. Differential requirements of Rab5 and Rab7 for endocytosis of influenza and other enveloped viruses. Traffic **4:**333–343.
37. **Simmons, G., D. N. Gosalia, A. J. Rennekamp, J. D. Reeves, S. L. Diamond, and P. Bates.** 2005. Inhibitors of cathepsin L prevent severe acute respiratory syndrome coronavirus entry. Proc. Natl. Acad. Sci. USA **102:**11876–11881.
38. **Sorkin, A.** 2004. Cargo recognition during clathrin-mediated endocytosis: a team effort. Curr. Opin. Cell Biol. **16:**392–399.
39. **Stang, E., F. D. Blystad, M. Kazazic, V. Bertelsen, T. Brodahl, C. Raiborg, H. Stenmark, and I. H. Madshus.** 2004. Cbl-dependent ubiquitination is required for progression of EGF receptors into clathrin-coated pits. Mol. Biol. Cell **15:**3591–3604.
40. **Sun, X., V. K. Yau, B. J. Briggs, and G. R. Whittaker.** 2005. Role of clathrin-mediated endocytosis during vesicular stomatitis virus entry into host cells. Virology **338:**53–60.
41. **Yang, Z. Y., Y. Huang, L. Ganesh, K. Leung, W. P. Kong, O. Schwartz, K. Subbarao, and G. J. Nabel.** 2004. pH-dependent entry of severe acute respiratory syndrome coronavirus is mediated by the spike glycoprotein and enhanced by dendritic cell transfer through DC-SIGN. J. Virol. **78:**5642–5650.
42. **Yao, D., M. Ehrlich, Y. I. Henis, and E. B. Leof.** 2002. Transforming growth factor-beta receptors interact with AP2 by direct binding to beta2 subunit. Mol. Biol. Cell **13:**4001–4012.
43. **Yu, F., M. Q. Le, S. Inoue, H. T. Thai, F. Hasebe, M. Del Carmen Parquet, and K. Morita.** 2005. Evaluation of inapparent nosocomial severe acute respiratory syndrome coronavirus infection in Vietnam by use of highly specific recombinant truncated nucleocapsid protein-based enzyme-linked immunosorbent assay. Clin. Diagn. Lab. Immunol. **12:**848–854.
44. **Ziebuhr, J.** 2004. Molecular biology of severe acute respiratory syndrome coronavirus. Curr. Opin. Microbiol. **7:**412–419.

Available online at www.sciencedirect.com
ScienceDirect
VIROLOGY
Virology 369 (2007) 198–205
www.elsevier.com/locate/yviro

Up-regulation of hepatitis C virus replication by human T cell leukemia virus type I-encoded Tax protein

Jing Zhang [a,*], Osamu Yamada [a], Kenji Kawagishi [a], Hiroshi Yoshida [a], Hiromasa Araki [a], Shoji Yamaoka [b], Toshio Hattori [c], Kunitada Shimotohno [d]

[a] *Research and Development Center, FUSO Pharmaceutical Industries, LTD., 2-3-30 Morinomiya, Joto-ku, Osaka 536-8523, Japan*
[b] *Department of Molecular Virology, Graduate School of Medicine, Tokyo Medical and Dental University, Tokyo 113-8519, Japan*
[c] *Department of Infectious and Respiratory Diseases, Tohoku University School of Medicine, Sendai, Japan*
[d] *Department of Viral Oncology, The Institute for Virus Research, Kyoto University, Kyoto 606-8397, Japan*

Received 22 June 2007; returned to author for revision 18 July 2007; accepted 31 July 2007
Available online 4 September 2007

Abstract

Co-infection of hepatitis C virus (HCV) with other blood-borne pathogens such as human T cell leukemia virus (HTLV) is common in highly endemic areas. Clinical evidence showing a correlation between HTLV-I co-infection and rapid progression of HCV-associated liver disease promoted us to investigate the effect of HTLV-I-encoded Tax protein on HCV replication. Reporter assay showed that HCV replicon-encoded luciferase expression was significantly augmented by co-transfection of the Tax-expressing plasmid. Further, HCV RNA replication in replicon cells was increased either by co-culture with cells stably expressing Tax protein (Huhtax) or by culture in the presence of Huhtax-conditioned medium, indicating that Tax could also modulate HCV replication of adjacent cells in a paracrine manner. Additionally, HCV replication in Huhtax exhibited a reduced responsiveness to interferon-α-induced antiviral activity. This study demonstrates the facilitation of HCV replication by Tax protein, which may partially account for severer clinical consequences of HCV-related disease in HCV/HTLV co-infected individuals.

Keywords: HCV; HTLV-I; Co-infection; Replication

Introduction

Hepatitis C virus (HCV) is the major causative agent of posttransfusional non-A, non-B viral hepatitis. Chronic HCV infection is frequently associated with liver cirrhosis and hepatocellular carcinoma (HCC), being a global health threat and the main cause of adult liver transplants in developed nations. HCV is a member of the Flaviviridae family with a positive-sense RNA genome of ~9600 nucleotides in length (Choo et al., 1989). The genome is flanked by highly structured nontranslated regions (NTRs) important for both RNA translation and replication. The viral genome encodes a polyprotein precursor of approximately 3010 amino acids, which is processed by viral and cellular protease to produce the structural proteins (core, E1 and E2) and nonstructural (NS) proteins (p7 and NS2 to NS5B) (Major and Feinstone, 1997).

Human T cell leukemia virus type I (HTLV-I) has been etiologically linked to the development of adult T cell leukemia/lymphoma (ATL) (Yoshida et al., 1984) and to chronic conditions including tropical spastic paraparesis/HTLV-I associated myelopathy (TSP/HAM) (Gessain et al., 1985; Osame et al., 1986). The HTLV-I genome encodes several regulatory proteins including Tax that are essential for viral replication. In addition to transcriptionally activating the promoter in 5′ long terminal repeat, Tax has also been shown to regulate the transcriptional activity of cellular promoters by serving as a transcriptional cofactor for the cyclic AMP-responsive element-binding factor (CREB), NF-κB, and the serum-responsive factor (SRF) pathways. Most of the cellular genes modulated by Tax are involved in growth, differentiation, apoptosis and cell cycle control.

HCV/HTLV-I co-infection is frequent in the regions that are highly endemic for both viral infections, probably due to the

* Corresponding author. Fax: +81 6 6964 2706.
E-mail address: j-zhang@fuso-pharm.co.jp (J. Zhang).

0042-6822/$ - see front matter © 2007 Elsevier Inc. All rights reserved.
doi:10.1016/j.virol.2007.07.032

similarity of the transmission route. Multiple lines of clinical evidence have shown that HCV co-infection with HTLV-I is associated with an increased risk of progression to severe liver disease and an elevated mortality due to liver cancer (Boschi-Pinto et al., 2000; Kishihara et al., 2001), highlighting the involvement of HTLV-I in HCV-related pathogenic processes. Although it is generally believed that the immunosuppressive effects of HTLV-I may exacerbate the progression of liver disease by attenuating the cytotoxic T lymphocyte response to HCV-infected hepatocytes, molecular interaction between HCV and HTLV-I might also play a role in the pathogenesis of severe liver disease.

In this study, we investigated possible interaction between HCV and HTLV-I. Our data indicate that HTLV-I-encoded Tax protein up-regulates the replication of HCV RNA in replicon cells and the Tax-mediated HCV activation was observed not only in Tax-expressing cells themselves but in those neighboring exposed cells as well.

Results

Activation of HCV replication by Tax

To investigate the possible influence of Tax protein on HCV replication, a human hepatoma cell line (Huh-7) was transfected with Tax-expressing plasmid (pCnwtax), and HCV replicon RNA in vitro transcribed from pLMH14, which contains the 5′ NTR, the first 36 nucleotides of the core region fused directly with the firefly luciferase reporter gene, the IRES element from encephalomyocarditis virus (EMCV) that directs translation of the HCV proteins from NS3 to NS5B and the 3′ NTR of HCV RNA (Fig. 1A) (Murata et al., 2005; Zhang et al., 2005b). The replicon-encoded luciferase expression, which was used as a read out of HCV RNA levels, was assayed at 3 and 72 h post-transfection. The luciferase levels at 3 h posttransfection were used to normalize the transfection efficiency. As shown in Fig. 1B, the luciferase expression from LMH14 replicon was sig-

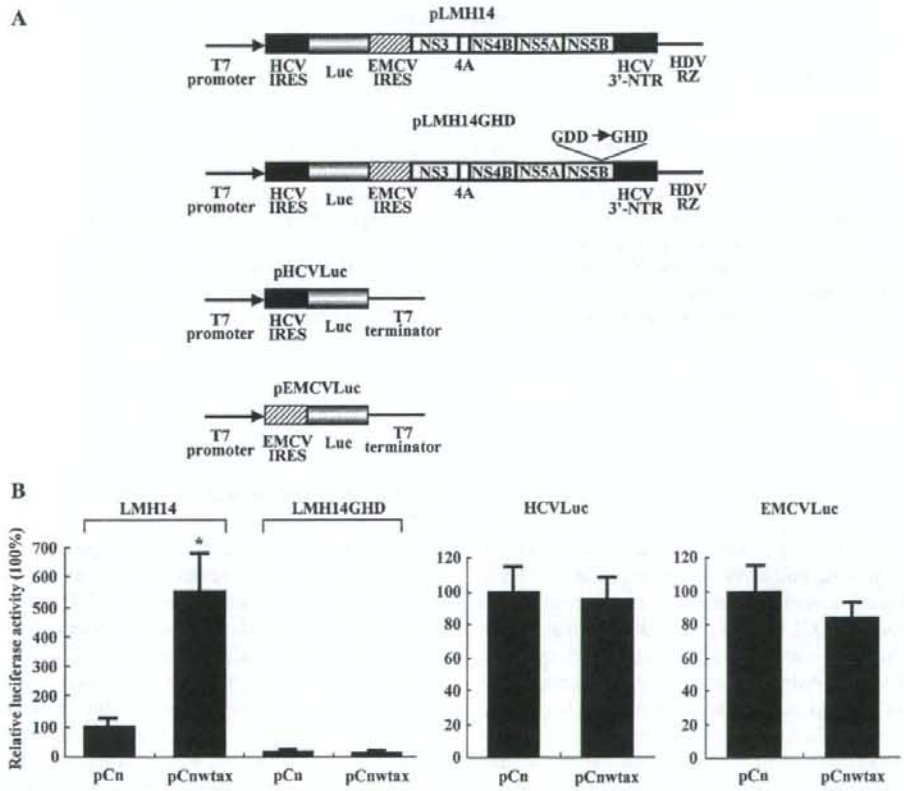

Fig. 1. Activation of HCV replication by HTLV-I Tax. (A) Schematic diagrams of the HCV replicon construct pLMH14, the replication-deficient replicon pLMH14GHD, as well as two control reporter vectors pHCVLuc and pEMCVLuc. pLMH14 contains T7 promoter, 5′ nontranslated region (NTR), the first 36 nucleotides of the core region fused directly with the firefly luciferase reporter gene, the internal ribosome entry site (IRES) element from encephalomyocarditis virus (EMCV) that directs translation of the HCV proteins from nonstructural (NS)3 to NS5B and the 3′ NTR of HCV RNA. pLMH14GHD is identical to pLMH14 except for carrying an inactive GHD motif in RdRp. pHCVLuc and pEMCVLuc contain the luciferase gene downstream of T7 promoter and HCV or EMCV IRES elements identical to that inserted in pLMH14, respectively. (B) The RNAs in vitro transcribed from the indicated vectors were transfected into Huh-7 cells together with pCn or pCnwtax-expressing Tax protein. Luciferase activities in the lysates were measured at 3 h and 72 h posttransfection. Luciferase activities at 3 h were used to normalize the transfection efficiency. Relative luciferase activity at 72 h in cells transfected with pCn was defined as 100%, and that in pCnwtax transfectant is expressed as relative percentage. The results are from five independent triplicate transfections. Luc, luciferase. $^{*}P<0.05$ compared with pCn.

nificantly enhanced in cells expressing Tax protein, being approximately five- to six-fold of that in cells transfected with the empty vector pCn (previously referred to as pCMV-NEO-BAM in Baker et al., 1990), whereas co-transfection of pCnwtax did not significantly affect the luciferase expression from replication-deficient replicon LMH14GHD, in which the catalytic GDD motif of NS5B polymerase was replaced by inactive GHD motif (Fig. 1A). In view of the structural characteristic of pLMH14, in which the luciferase gene is synthesized under the control of HCV IRES and the NS proteins are initiated by EMCV IRES, thus up-regulation of HCV IRES- and/or EMCV IRES-mediated translation may also lead to an enhanced luciferase expression from LMH14 replicon. To investigate whether the augmentation of luciferase expression by Tax was due to its influence on HCV IRES- or EMCV IRES-dependent translation, we performed reporter assays with the RNA in vitro transcribed from reporter vectors pHCVLuc and pEMCVLuc (Fig. 1A), in which the expression of reporter gene is directed by HCV IRES and EMCV IRES elements identical to those inserted in pLMH14, respectively. Neither HCV IRES- nor EMCV IRES-directed luciferase expression was significantly affected by co-transfection of pCnwtax, indicating that the observed increment in luciferase expression was due to an enhancing effect of Tax on HCV replication rather than to its influence on HCV IRES- or EMCV IRES-mediated translation. Taken together, these results suggest that HTLV-I Tax protein enhances the replication of HCV replicon.

The molecular mechanism underlying Tax-mediated HCV activation

Tax protein has been shown to exert its biological activities through distinct pathways: it activates HTLV-I transcription through CREB/ATF, induces transcription of HIV, IL-2, IL-2Rα, GM-CSF and expression of the cellular immediate early genes via NF-κB and SRF pathways, respectively. To explore the molecular mechanism underlying Tax-mediated activation of HCV replication, two Tax mutant-expressing plasmids, pCnm148 and pCnm319, were employed in transient transfection experiments (Yamaoka et al., 1996). m148 (G148V) retains the ability to activate CREB/ATF pathway while failing to activate NF-κB pathway. Conversely, m319 (L319R and L320S) was shown to be functional in activating NF-κB pathway while lacks the ability to activate CREB/ATF pathway. As expected, reporter gene expression under the control of HTLV-I LTR promoter was enhanced substantially by co-transfetion with plasmid expressing wild-type Tax (wtax) or m148, but only moderately by m319 (Fig. 2A, upper), on the other hand, HIV-I LTR-directed luciferase expression was significantly increased by co-transfetion with plasmid expressing wtax or m319, but not by m148 (Fig. 2A, middle).

To compare the effects of wtax, m148 and m319 on HCV replication, plasmid expressing wild- or mutant-type Tax was transfected into Huh-7 cells together with the replicon RNA in vitro transcribed from pLMH14, and the replicon-encoded luciferase activities were measured as described above. As

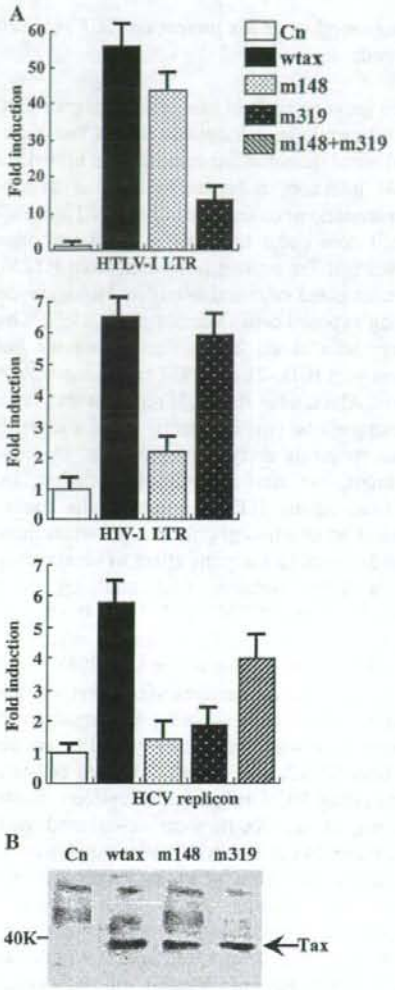

Fig. 2. Effect of Tax or its mutants on HCV replication. (A) Huh-7 cells were transfected with pHTLVLTR-Luc (upper), pHIVLTR-Luc (middle) or the replicon RNA in vitro transcribed from pLMH14 (lower), along with pCn, pCnwtax, pCnm148 or pCnm319. Relative luciferase activities were determined as described for Fig. 1. Fold induction means the luciferase activity relative to that co-transfected with the empty vector pCn. The results are from four independent triplicate experiments. (B) Expression of Tax protein in each transfectant was confirmed by Western blot analysis. Solid arrow indicates the signals of Tax protein.

shown in Fig. 2A (lower), Tax-mediated enhancement of HCV replication was significantly abrogated either by mutation incorporated in m148 or those in m319. Interestingly, co-expression of m148 and m319 restored the replicon-encoded reporter gene expression to some extent. This result suggests that both NF-κB- and CREB-dependent pathways may be involved in Tax-mediated activation of HCV RNA replication. In these experiments, expression of wild- or mutant-type Tax protein was confirmed by Western blot analysis, and the representative result is shown in Fig. 2B.

The paracrine effect of Tax protein on HCV replication in adjacent cells

While a growing body of evidence has shown that HCV can replicate efficiently in extrahepatic tissues and cells including peripheral blood mononuclear cells, there is little demonstration of HTLV-I infection in hepatic cells. It is thus not certain whether a scenario of co-infection of HTLV-I and HCV in same hepatic cell does occur in dually infected individuals. It has been shown that Tax protein is released from HTLV-I-infected and Tax-transfected cells and exerts its biological activities in neighboring exposed cells (Marriott et al., 1992; Cowan et al., 1997; Szymocha et al., 2000). Further, on the basis of the observation with BHK-21 and 293T cells transiently expressing Tax protein, Alefantis et al. (2005) reported that Tax is released into the extracellular environment by cellular secretion process other than apoptosis or lysis of the cells. In view of these considerations, we next investigated whether Tax protein released from certain HTLV-I-infected cells could modulate HCV replication of adjacent cells in a paracrine manner. MT-2 cells provide a tool to study the effect of paracrine-acting Tax, however, a lesson obtained from studying the molecular interaction between HTLV-I and HIV showed that MT-2 supernatant additionally contains multiple factors with adverse effect on HIV infection (Moriuchi et al., 1998), which makes it difficult to investigate the authentic effect of soluble Tax. Accordingly, instead of MT-2 cells, we employed Huh-7 cells stably expressing wild- or mutant-type Tax protein for this purpose. Huh-NNRZ cells, a Huh-7-derived cell line constitutively replicating HCV subgenomic replicon (Kishine et al., 2002; Zhang et al., 2004), were co-cultured with HuhCn, Huhwtax, Huhm148 or Huhm319 cells, which were established by transfection with pCn, pCnwtax, pCnm148 or pCnm319 followed by G418 selection. Similar level of Tax expression in each cell line was confirmed by Western blot analysis (Fig. 3A). Three days later, total RNAs were extracted and subjected to real-time RT-PCR for quantification of HCV replicon RNA levels. As shown in Fig. 3B, HCV RNA was significantly increased in Huh-NNRZ cells co-cultured with Huhwtax, being approximately 6-fold higher than that co-cultured with HuhCn, while co-culture with Huhm148 or Huhm319 did not obviously affect the HCV RNA level in replicon cells. Similar result was also obtained when Huh-NNRZ cells were incubated in the presence of 50% supernatant from Huhwtax cell culture (Fig. 3C). Moreover, pretreatment with anti-Tax antibody reduced, although did not abolish completely, the ability of Huhwtax-conditioned medium to activate HCV replication, confirming a specific role of Tax in the enhanced HCV replication. The fact that the stimulatory activity was partially retained even after treatment with anti-Tax antibody may be attributable to the enhancing effect of other soluble factors pre-induced by Tax in the conditioned medium. Indeed, it was reported that the activation of CMV replication by Tax protein is largely mediated by induction of interleukin-8 and transforming growth factor-β (Szabo et al., 1999).

To further confirm that Tax protein could affect HCV replication in a paracrine manner, we next examined the effect of

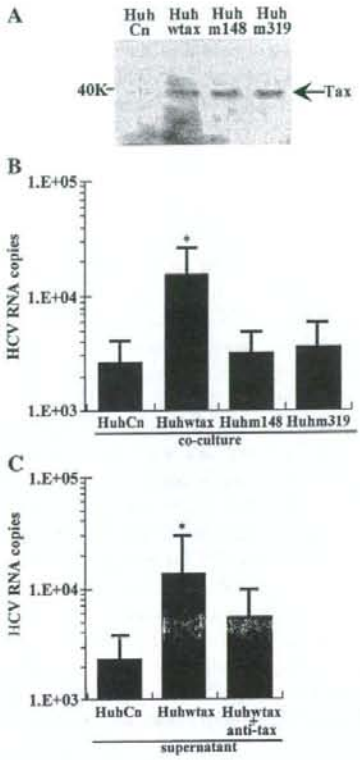

Fig. 3. Paracrine effect of HTLV-1 Tax on HCV replication. (A) Similar level of Tax expression in cell lines stably expressing wild- or mutant-type Tax. Huh-7 cells were transfected with pCn, pCnwtax, pCnm148 or pCnm319 followed by G418 selection, and Tax expression was detected by Western blot analysis. Huh-NNRZ cells were co-cultured with the indicated stable cell lines (B) or were incubated in the presence of 50% culture supernatants from HuhCn or Huhwtax pretreated with or without anti-Tax (C). After a 3-day culture, the cells were harvested and HCV replicon RNAs were quantified with real-time RT-PCR. GAPDH mRNA level in each sample was simultaneously quantified to normalize the value of HCV replicon RNA. Representative data are from three separate experiments. $^{*}P<0.05$ compared with HuhCn.

recombinant Tax protein expressed in *Escherichia coli* on HCV replication. GST-Tax was purified and added to the culture of Huh-7 cells transfected with HCV replicon RNA at 3 h posttransfection. After an additional 72 h, the replicon-encoded luciferase activities were measured and corrected by those determined at 3 h posttransfection. As shown in Fig. 4B, incubation of Huh-7 cells in the presence of 5 nM GST-Tax protein, but not of GST protein, resulted in an enhanced replication of HCV replicon. Together with the results described above, the data demonstrate that Tax protein could also up-regulate HCV replication in neighboring exposed cells.

Modulation of interferon-α-induced antiviral activity by Tax

Next we were interested in investigating whether Tax alters the responsiveness of HCV replication to interferon (IFN)-α. To this end, Huhwtax and HuhCn cells were transfected with the replicon RNA in vitro transcribed from pLMH14. Cells were

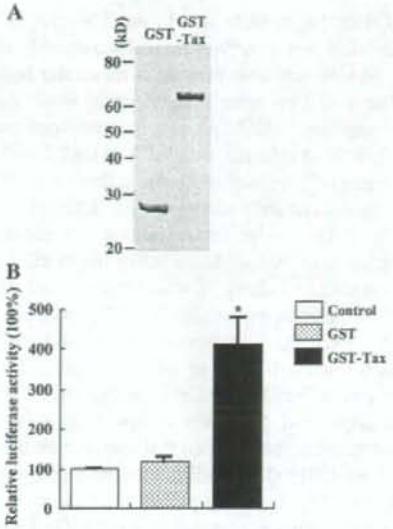

Fig. 4. Up-regulation of HCV replication by recombinant Tax protein. (A) SDS-PAGE analysis of purified GST and GST-Tax proteins. The gel was stained with Coomassie blue. (B) Huh-7 cells transfected with replicon RNA was cultured in the absence or presence of 5 nM GST, or GST-Tax for 72 h, and the relative luciferase activities in the lysates were determined as described for Fig. 1. The results are from two independent triplicate transfections. $*P<0.05$ compared with control.

harvested and divided into several aliquots, which were further incubated for 3 days in the presence of various IFN-α concentrations ranging from 0.3 to 100 IU/ml. The corrected replicon-encoded luciferase activities were shown in Fig. 5A. At each IFN concentration, luciferase activity detected in Huhwtax was significantly higher than that in HuhCn, and the difference was more significant with the increase of IFN concentration. Although a similar dose-dependent manner was observed, the IFN-α responsiveness of HCV replication in Huhwtax cells was poorer than that in HuhCn cells, with a 50% inhibitory concentration (IC_{50}) of about 3 to 10 IU/ml and 10 to 30 IU/ml, respectively.

Additionally, it was reported that HCV replication was highly dependent on cellular proliferation, both viral RNA and protein syntheses were largely increased in actively growing cells (Pietschmann et al., 2001; Scholle et al., 2004). To investigate whether the stimulatory effect of Tax on HCV replication was mediated by its influence on cell proliferation, growth characteristics for Huhwtax and HuhCn cells were analyzed. Expression of Tax protein did not significantly affect cell growth of Huh-7 cells, as evidence by similar growth curve was delineated for Huhwtax to that for HuhCn (Fig. 5B). This observation thus rules out the possibility that Tax up-regulates HCV replication via stimulating host cell growth.

Discussion

In this study, we have demonstrated that HTLV-I Tax protein up-regulates HCV replication, and this activation is not only limited in Tax-expressing cells but extended to those exposed neighboring cells. The latter is probably more important, considering that it is not certain whether co-infection of HTLV-I and HCV in same hepatic cells is possible in vivo because hepatic cells are not known as typical target cells for HTLV-1. With this respect, results presented in Figs. 1 and 2 may be of less clinical relevance because the experimental setting required co-infection of HTLV-1 and HCV in same target cells, however, these results provided important mechanistic information, which promoted us to further investigate the paracrine effect of Tax on HCV replication. Tax has been shown to be released from infected cells, and extracellular Tax has been reported to play pathological roles in multiple HTLV-1-associated diseases. For example, it was demonstrated that extracellular HTLV-I Tax activated the expression of endogenous IL-2Rα in lymphocyte, being a causative factor of the abnormal lymphocyte proliferation observed in ATL and TSP (Marriott et al., 1992). Also, it was reported that extracellular Tax induced TNF-α expression in neuronal cells (Cowan et al., 1997) and impaired the ability of astrocytes to manage the steady-state level of glutamate (Szymocha et al., 2000), both of which may contribute to the pathogenesis of HTLV-1-associated TSP. We

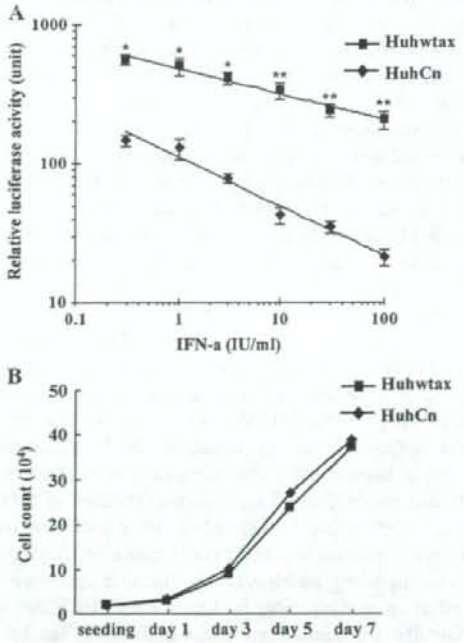

Fig. 5. (A) Modulation of interferon (IFN)-α responsiveness of HCV replication by HTLV-I Tax. HuhCn or Huhwtax cells were transfected with the replicon RNA in vitro transcribed from pLMH14, harvested and divided into several aliquots at 3 h posttransfection, which were further incubated for 3 days in the presence of various IFN-α concentrations ranging from 0.3 to 100 IU/ml. Replicon-encoded luciferase activity was measured and corrected by that determined at 3 h posttransfection. Representative results from three independent experiments are shown. $*P<0.05$ $**P<0.01$ compared with HuhCn. (B) Expression of Tax does not affect cell growth. HuhCn or Huhwtax cells were seeded at 2×10^4 cells per well in 24-well plates and were counted on the following days as indicated.

now extended this list by showing up-regulating effect of extracellular Tax on replication of co-infected HCV, which may consequently contribute to the pathogenesis of severe HCV-related diseases in HCV/HTLV co-infected individuals. However, to make the conclusion more physiologically relevant, one issue remaining to be addressed is whether the Tax protein secreted from hepatic cells is same as that from naturally infected T cells. Further investigation is under way to clarify whether the Tax protein secreted from infected T cells exerts a similar biological behavior in stimulating HCV replication. Additionally, it was demonstrated that extracellular Tax protein enhanced HIV-1 fusion/entry, probably by transactivating the expression of cellular co-receptors such as CXCR4 and CCR5 (Moriuchi et al., 1998). The subgenomic replicon used here constructively lacks the core to NS2 region, making it impossible to study the complete HCV life cycle including entry, assembly and release of viral particles. Thus, the effect of Tax on HCV replication in vivo may be more complicated than those observed here.

Several pathogenic viruses, such as HIV (De Rossi et al., 1991; Siekevitz et al., 1987), CMV (Moch et al., 1992; Szabo et al., 1998; Toth et al., 1995), SV40 (Nakamura et al., 1989) and JC viruses (Okada et al., 2000), have been reported to be activated by Tax through transcriptional activation of viral genes. HCV is a positive-stranded RNA virus, fulfilling its replication process in cytoplasm. So it is apparent that Tax activates HCV replication via a distinct mechanism, probably by transactivating the expression of cellular genes involved in HCV replication and/or by induction of 'pro-HCV' factors providing favorable circumstance for viral replication. Consistent with this hypothesis, it was found that treatment of Huhtax-conditioned medium with anti-Tax antibody did not fully abolish its stimulatory effect on HCV replication, the partially retained enhancing effect may be attributable to the pre-existing Tax-induced soluble factors in the culture supernatant. Whether mediated directly or indirectly by other factors, Tax, especially the paracrine-acting Tax, may play an important role in the pathogenesis of severe HCV-related disease in patients dually infected with HCV and HTLV-I. We showed by reporter assay that the ability of Tax to stimulate HCV replication was abrogated in Tax mutants incompetent to activate either NF-κB- or CREB-dependent pathway, and co-expression of these two mutants, however, largely restored the HCV activation by Tax. These results suggest that the downstream effective factors of these two signaling pathways may function in concert with each other in participating in Tax-induced HCV activation. Alternatively, the stimulatory effect of HTLV-I Tax on HCV replication may be mediated by a single factor which is transactivated by Tax via concurrently acting on NF-κB and CREB-responsive elements. Indeed, it was reported that both NF-κB and CREB pathways are essential for significant activation of anti-apoptotic gene *Bcl-xl* in human cells (Mori et al., 2001). Further experiments are required to distinguish these possibilities.

In addition to its direct activation of HCV replication, Tax may also contribute to rapid progression of HCV-associated liver disease by modulating the antiviral activity of IFN-α. Compared with that in HuhCn, a lower IFN responsiveness of HCV replication was observed in Huhwtax stably expressing Tax (Fig. 5A), which may provide a molecular basis for the clinical observation showing a significantly lower rate of sustained IFN response in HCV patients with concomitant HTLV-I infection than those infected with HCV alone (Kishihara et al., 2001). The precise mechanism for the influence of Tax on IFN responsiveness is currently unknown. When tested in a reporter assay with ISRE *cis*-luciferase vector, co-transfection of pCnwtax inhibited IFN-α-induced activation of ISRE promoter (authors' unpublished data). It was demonstrated that adenovirus E1A oncoprotein suppresses Jak-STAT pathway by interacting with CBP/p300 co-activators and consequently inhibiting the recruitment of them to STAT proteins (Look et al., 1998). Tax also utilizes CBP/p300 co-activators for implementing its transcriptional activation competence, it is thus conceivable but remains to be proven that competition between Tax and STAT1 for CBP/p300 binding may be responsible for the attenuated Jak-STAT signaling pathway by Tax protein. If this is the case, exogenous expression of CBP/p300 would restore the reduced IFN responsiveness by Tax. Additionally, it was reported that IFN-induced protein kinase PKR could phosphorylate HIV-1 Tat, and Tat inhibited the activity of PKR both by blocking its ability to autophosphorylate in response to dsRNA and by competing with its natural substrate eIF2 (Brand et al., 1997). Both Tat and Tax activate NF-κB pathway by stimulating the phosphorylation and degradation of IκB, which has been shown to be one of the substrates of PKR; thus such a mutual interaction may also be possible between Tax and PKR. Studies are under way to further define the molecular mechanism for Tax-conferred IFN-resistance.

Additionally, it has been shown that inclusion of the fusion protein (GST) to the N-terminal of foreign gene may interfere with the biochemical activity of some recombinant protein, probably by spatial hindrance. For example, it was reported that fusion of GST at the N-terminal of the eukaryotic DNA-binding protein, RSRFC4, could not be tolerated (Sharrocks, 1994). The GST-Tax used here, however, was shown to be biologically active, as evidenced by the data revealed in Fig. 4 and those reported by Moriuchi et al. (1998) and Moriuchi and Moriuchi (2006), by whom the pGST-Tax plasmid was kindly provided.

We investigated here the molecular interaction between HCV and HTLV-I, and provided evidence demonstrating that HTLV-I-encoded Tax protein up-regulates replication of HCV. Our findings suggest that HTLV-I may accelerate the clinical progression of HCV-related disease in dually infected patients by Tax-mediated enhancement of HCV replication, although dysfunction of cellular immune response by HTLV-I may also play a role.

Materials and methods

Plasmids

Parental plasmid pCn is identical to pCMV-NEO-BAM described elsewhere (Baker et al., 1990). Plasmids encoding

wild-type HTLV Tax (pCnwtax) or its mutants (pCnm148 and pCnm319) were described in the previous report (Yamaoka et al., 1996).

Cells

The cell line Huh-7 was purchased from the American Type Culture Collection (ATCC) and maintained in Dulbecco's modified Eagle's medium (DMEM, Invitrogen) supplemented with 10% fetal calf serum and 50 U/ml penicillin and streptomycin in a 5% CO_2 humidified atmosphere. The cell lines Huhwtax, Huhm148 and Huhm319, which stably express wild- or mutant-type Tax protein, were established by transfecting Huh-7 cells with pCnwtax, pCnm148 or pCnm319, followed by selection in the presence of 600 μg/ml G418 (Geneticin, Invitrogen). A Huh-7-derived cell line (Huh-NNRZ) stably replicating HCV subgenomic replicon was grown in DMEM medium containing 300 μg/ml G418 (Kishine et al., 2002; Zhang et al., 2004).

Preparation of recombinant Tax protein

GST-Tax fusion protein was induced by isopropyl-thiogalactopyranoside in *E. coli* DH5a cells transformed with pGST-Tax (Moriuchi et al., 1998), purified by binding to glutathione-Sepharose 4B (Bulk GST Purification Module, GE Healthcare), and recovered by elution with 10 mM reduced glutathione.

In vitro transcription

For synthesis the replicon RNA, pLMH14 or pLMH14GHD was linearized at *Xba*I site located immediately downstream of the HDV ribozyme, and then transcribed in vitro using T7 RNA polymerase according to the protocol supplied by the manufacturer (Roche). After transcription, 10 U of RQ DNase I (Promega) was added to the reaction mixture to digest DNA templates. The mixture was extracted with phenol–chloroform and RNA was precipitated with ethanol–7.5 M ammonium acetate.

Transfection

Huh-7 cells were seeded at 1×10^5 per well of 12-well plates 24 h before transfection. 0.5 μg of replicon RNA in vitro transcribed from pLMH14 or pLMH14GHD, and 1 μg of pCnwtax, pCnm148 or pCnm319 were co-transfected into cells with Lipofectin Reagent (Invitrogen). The cells were harvested and the luciferase activity was determined at 3 h and 72 h posttransfection as described below. The luciferase level at 3 h posttransfection was used to correct transfection efficiency.

Luciferase assay

Cell lysates were prepared from transfected cells, centrifuged briefly, and 20 μl of the supernatants was used for luciferase assays. Luciferase activity was measured using a TD-20/20 Luminometer (Promega).

Western blot analysis

Protein was electrophoresed on a sodium dodecyl sulfate-polyacrylamide gel, transferred to Hybond-P PVDV Membrane (GE Healthcare). The blot was probed with monoclonal antibody specific for HTLV-I Tax (AS-5703, Microbix Biosystems Inc.), and signals were visualized with ECL Plus Western Blotting Detection Reagents (GE Healthcare).

Real-time RT-PCR

RNAs were isolated from cultured cells with Trizol reagent (Invitrogen) and HCV replicon RNA was quantified by real-time RT-PCR as described previously (Zhang et al., 2005a). Briefly, 1 μg of DNase-treated total RNA was reserve transcribed and subsequently amplified with SYBR GREEN according to the protocol supplied by the manufacturer (Takara). Glyceraldehyde-3-phosphate dehydrogenase (GAPDH) mRNA level in each sample was simultaneously quantified to normalize the value of HCV replicon RNA.

References

Alefantis, T., Mostoller, K., Jain, P., Harhaj, E., Grant, C., Wigdahl, B., 2005. Secretion of the human T cell leukemia virus type I transactivator protein Tax. J. Biol. Chem. 280 (17), 17353–17362.

Baker, S.J., Markowitz, S., Fearon, E.R., Willson, J.K.V., Vogelstein, B., 1990. Suppression of human colorectal carcinoma cell growth by wild-type p53. Science 249 (4971), 912–915.

Boschi-Pinto, C., Stuver, S., Okayama, A., Trichopoulos, D., Orav, E.J., Tsubouchi, H., Mueller, N., 2000. A follow-up study of morbidity and mortality associated with hepatitis C virus infection and its interaction with human T lymphotropic virus type I in Miyazaki, Japan. J. Infect. Dis. 181 (1), 35–41.

Brand, S.R., Kobayashi, R., Mathews, M.B., 1997. The Tat protein of human immunodeficiency virus type 1 is a substrate and inhibitor of the interferon-induced, virally activated protein kinase, PKR. J. Biol. Chem. 272 (13), 8388–8395.

Choo, Q.L., Kuo, G., Weiner, A.J., Overby, L.R., Bradley, D.W., Houghton, M., 1989. Isolation of a cDNA clone derived from a blood-borne non-A, non-B viral hepatitis C virus genome. Science 244 (4902), 359–362.

Cowan, E.P., Alexander, R.K., Daniel, S., Kashanchi, F., Brady, J.N., 1997. Induction of tumor necrosis factor alpha in human neuronal cells by extracellular human T-cell lymphotropic virus type 1 Tax1. J. Virol. 71 (9), 6982–6989.

De Rossi, A., Saggioro, D., Calabro, M.L., Cenzato, R., Chieco-Bianchi, L., 1991. Reciprocal activation of human T-lymphotropic viruses in HTLV-I-transformed cells superinfected with HIV-1. J. Acquir. Immune Defic. Syndr. 4 (4), 380–385.

Gessain, A., Barin, F., Vernant, J.C., Gout, O., Maurs, L., Calender, A., de The, G., 1985. Antibodies to human T-lymphotropic virus type-I in patients with tropical spastic paraparesis. Lancet 2 (8452), 407–410.

Kishihara, Y., Furusyo, N., Kashiwagi, K., Mitsutake, A., Kashiwagi, S., Hayashi, J., 2001. Human T lymphotropic virus type 1 infection influences hepatitis C virus clearance. J. Infect. Dis. 184 (9), 1114–1119.

Kishine, H., Sugiyama, K., Hijikata, M., Kato, N., Takahashi, H., Noshi, T., Nio, Y., Hosaka, M., Miyanari, Y., Shimotohno, K., 2002. Subgenomic replicon derived from a cell line infected with the hepatitis C virus. BBRC 293 (3), 993–999.

Look, D.C., Roswit, W.T., Frick, A.G., Gris-Alevy, Y., Dickhaus, D.M., Walter, M.J., Holtzman, M.J., 1998. Direct suppression of stat1 function during adenoviral infection. Immunity 9 (6), 871–880.

Major, M.E., Feinstone, S.M., 1997. The molecular virology of hepatitis C. Hepatology 25 (6), 1527–1538.

Marriott, S.J., Trinh, D., Brady, J.N., 1992. Activation of interleukin-2 receptor alpha expression by extracellular HTLV-I Tax1 protein: a potential role in HTLV-I pathogenesis. Oncogene 7 (9), 1749–1755.

Moch, H., Lang, D., Stamminger, T., 1992. Strong trans activation of the human cytomegalovirus major immediate-early enhancer by $p40^{tax}$ of human T-cell leukemia virus type I via two repetitive Tax-responsive sequence elements. J. Virol. 66 (12), 7346–7354.

Mori, N., Fujii, M., Cheng, G., Ikeda, S., Yamasaki, Y., Yamada, Y., Tomonaga, M., Yamamoto, N., 2001. Human T-cell leukemia virus type I tax protein induces the expression of anti-apoptotic gene Bcl-xL in human T-cells through nuclear factor-kappaB and c-AMP responsive element binding protein pathways. Virus Genes 22 (3), 279–287.

Moriuchi, M., Moriuchi, H., 2006. Induction of lactoferrin gene expression in myeloid or mammary gland cells by human T-cell leukemia virus type 1 (HTLV-1) Tax: implication for milk-borne transmission of HTLV-1. J. Virol. 80 (14), 7118–7126.

Moriuchi, H., Moriuchi, M., Fauci, A.S., 1998. Factors secreted by human T lymphotropic virus type I (HTLV-I)-infected cells can enhances or inhibit replication of HIV-1 in HTLV-I-uninfected cells: implication for in vivo coinfection with HTLV-I and HIV-1. J. Exp. Med. 187 (10), 1689–1697.

Murata, T., Ohshima, T., Yamaji, M., Hosaka, M., Miyanari, Y., Hijikata, M., Shimotohno, K., 2005. Suppression of hepatitis C virus replicon by TGF-β. Virology 331 (2), 407–417.

Nakamura, M., Niki, M., Nagata, K., Ohtani, K., Saito, S., Hinuma, Y., Sugamura, K., 1989. Cell line-dependent response of the enhancer element of simian virus 40 to transactivator p40tax encoded by human T-cell leukemia virus type I. J. Biol. Chem. 264 (34), 20189–20192.

Okada, Y., Sawa, H., Tanaka, S., Takada, A., Suzuki, S., Hasegawa, H., Umemura, T., Fujisawa, J., Tanaka, Y., Hall, W.W., Nagashima, K., 2000. Transcriptional activation of JC virus by human T-lymphotropic virus type I Tax protein in human neuronal cell lines. J. Biol. Chem. 275 (22), 17016–17023.

Osame, M., Usuku, K., Izumo, S., Ijichi, N., Amitani, H., Igata, A., 1986. HTLV-I associated myelopathy, a new clinical entity. Lancet 1 (8488), 1031–1032.

Pietschmann, T., Lohmann, V., Rutter, G., Kurpanek, K., Bartenschlager, R., 2001. Characterization of cell lines carrying self-replicating hepatitis C virus RNAs. J. Virol. 75 (3), 1252–1264.

Scholle, F., Li, K., Bodola, F., Ikeda, M., Luxon, B.A., Lemon, S.M., 2004. Virus-host cell interactions during hepatitis C virus RNA replication: impact of polyprotein expression on the cellular transcriptome and cell cycle association with viral RNA synthesis. J. Virol. 78 (3), 1513–1524.

Sharrocks, A.D., 1994. A T7 expression vector for producing N- and C-terminal fusion proteins with glutathione S-transferase. Gene 138 (1-2), 105–108.

Siekevitz, M., Josephs, S.F., Dukovich, M., Peffer, N., Wong-Staal, F., Greene, W.C., 1987. Activation of the HIV-1 LTR by T cell mitogens and the trans-activator protein of HTLV-I. Science 238 (4833), 1575–1578.

Szabo, J., Bacsi, A., Andirko, I., Kiss, J., Nemes, J., Toth, F.D., 1998. Reciprocal interactions between human cytomegalovirus and human T cell leukemia–lymphoma virus type I in monocyte-derived macrophages cultured in vitro. AIDS Res. Hum. Retrovir. 14 (8), 699–709.

Szabo, J., Bacsi, A., Beck, Z., Kiss, J., Andirko, I., Toth, F.D., 1999. Role of interleukin-8 and transforming growth factor-beta1 in enhancement of human cytomegalovirus replication by human T cell leukemia–lymphoma virus type I in macrophages coinfected with both viruses. J. Interferon Cytokine Res. 19 (2), 209–217.

Szymocha, R., Akaoka, H., Dutuit, M., Malcus, C., Didier-Bazes, M., Belin, M.F., Giraudon, P., 2000. Human T-cell lymphotropic virus type 1-infected T lymphocytes impair catabolism and uptake of glutamate by astrocytes via Tax-1 and tumor necrosis factor alpha. J. Virol. 74 (14), 6433–6441.

Toth, F.D., Aboagye-Mathiesen, G., Szabo, J., Liu, X., Mosborg-Petersen, P., Kiss, J., Hager, H., Zdravkovic, M., Andirko, I., Aranyosi, J., 1995. Bidirectional enhancing activities between human T cell leukemia–Lymphoma virus type I and human cytomegalovirus in human term syncytiotrophoblast cells cultured in vitro. AIDS Res. Hum. Retrovir. 11 (12), 1495–1507.

Yamaoka, S., Inoue, H., Sakurai, M., Sugiyama, T., Hazama, M., Yamada, T., Hatanaka, M., 1996. Constitutive activation of NF-kB is essential for transformation of rat fibroblasts by the human T-cell leukemia virus type I Tax protein. EMBO J. 15 (4), 873–887.

Yoshida, M., Seiki, M., Yamaguchi, K., Takatsuki, K., 1984. Monoclonal integration of human T-cell leukemia provirus in all primary tumors of adult T-cell leukemia suggests causative role of human T-cell leukemia virus in the disease. Proc. Natl. Acad. Sci. U.S.A. 81 (19), 2534–2537.

Zhang, J., Yamada, O., Sakamoto, T., Yoshida, H., Iwai, T., Matsushita, Y., Shimamura, H., Araki, H., Shimotohno, K., 2004. Down-regulation of viral replication by adenoviral-mediated expression of siRNA against cellular cofactors for hepatitis C virus. Virology 320 (1), 135–143.

Zhang, J., Yamada, O., Sakamoto, T., Yoshida, H., Araki, H., Shimotohno, K., 2005a. Exploiting cis-acting replication elements to direct hepatitis C virus-dependent transgene expression. J. Virol. 79 (10), 5923–5932.

Zhang, J., Yamada, O., Sakamoto, T., Yoshida, H., Araki, H., Murata, T., Shimotohno, K., 2005b. Inhibition of hepatitis C virus replication by pol III-directed overexpression of RNA decoys corresponding to stem-loop structures in the NS5B coding region. Virology 342 (2), 276–285.

Images in *Thorax*

Secondary bronchiolitis obliterans organising pneumonia in a patient with carbamazepine-induced hypogammaglobulinemia

A 49-year-old woman had been treated with carbamazepine for 2 years because of epilepsy. She was referred to us for progressive exertional dyspnea and prolonged productive cough. Chest computed tomography (CT) scan showed bilateral infiltrates including ground glass opacities and consolidations predominantly in the lower lung fields. Her laboratory findings showed severe hypogammaglobulinemia, that is, immunoglobulin (Ig) G 418 mg/dl (normal, 748–1694 mg/dl), Ig A 20 mg/dl (91–391 mg/dl) and Ig M 51 mg/dl (33–254 mg/dl). Carbamazepine and other suspected antibiotics were all negative for drug-induced lymphocyte stimulation tests. Histological examination by trans-bronchial lung biopsy showed intraluminal fibrosis of distal airspaces with foamy alveolar macrophages, suggesting bronchiolitis obliterans organising pneumonia (BOOP). After the cessation of carbamazepine, all abnormalities in gammaglobulins and roentgenogram findings gradually improved without any medication. This good clinical course also considerably supports the diagnosis of BOOP.

BOOP may result from diverse causes such as drugs, acute respiratory infections and radiation treatment, or appear idiopathically.[1 2] Here, we show a case of secondary BOOP, which was associated with repeated respiratory infections caused by carbamazepine-induced hypogammaglobulinemia. Although the exact mechanisms of carbamazepine-induced hypogammaglobulinemia are unknown, they can be classified into three groups, that is, an absence of B cells,[3] an extensive impairment of the synthesis of Igs in B cells[3] and a disorder of the class-switch of Igs in B cells.[4] Our case described above would belong to the second group. Generally, drug-induced BOOP often develops within several weeks or less. However, our report indicates that even in the case of several years after use, anticonvulsants such as carbamazepine may have some adverse effects on the immune system and cause frequent airway infections, resulting in the development of secondary BOOP.

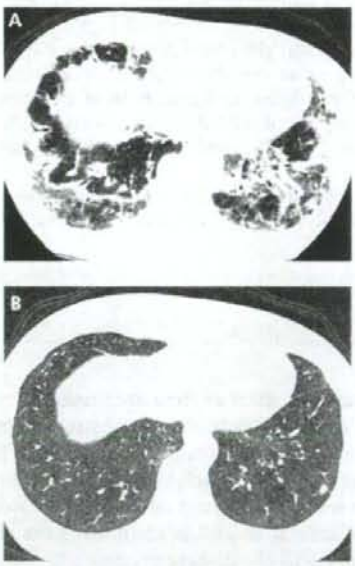

Figure 1 (A) Chest CT scans on admission. Bilateral infiltrates including ground glass opacities and consolidations are seen predominantly in lower lung fields. (B) Chest CT scans seven months after the cessation of carbamazepine showing marked improvement. The serum levels of Ig G, Ig A and Ig M are also increased to 1328, 69 and 355 mg/dl, respectively.

Learning points

- A drug-induced hypogammaglobulinemia after long term use of carbamazepine is very rare.
- A hypogammaglobulinemia should be considered as one of the causes of secondary bronchiolitis obliterans organising pneumonia with repeated airway infections.

ACKNOWLEDGEMENTS

The authors acknowledge Mr Brent K. Bell for reading the manuscript.

T Tamada, M Nara, M Tomaki, Y Ashino, T Hattori,
Division of Infectious and Respiratory Diseases, Department of Internal Medicine, Tohoku University Hospital, Sendai, Japan

Correspondence to: Tsutomu Tamada, Division of Infectious and Respiratory Diseases, Department of Internal Medicine, Tohoku University Hospital, Seiryo-machi, Aoba-ku, Sendai 980-8574, Japan; tamada@rid.med.tohoku.ac.jp

doi: 10.1136/thx.2006.063842

Competing interests: None declared.

REFERENCES

1 **Cordier J-F**. Organising pneumonia. *Thorax* 2000;**55**:318–28.
2 **Cazzato S**, Zompatori M, Baruzzi G, *et al*. Bronchiolitis obliterans-organizing pneumonia: an Italian experience. *Respir Med* 2000;**94**:702–8.
3 **Castro AP**, Redmershi MG, Pastorino AC, *et al*. Secondary hypogammaglobulinemia after use of carbamazepine: case report and review. *Rev Hosp Clin Fac Med Sao Paulo* 2001;**56**(6):189–92.
4 **Go T**. Carbamazepine-induced IgG1 and IgG2 deficiency associated with B cell maturation defect. *Seizure* 2004;**13**:187–90.

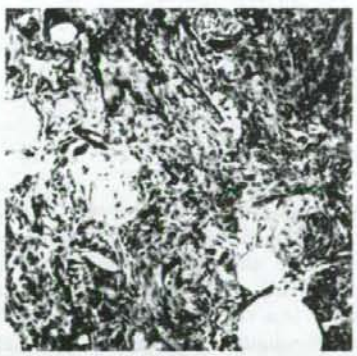

Figure 2 Elastica-Masson staining of specimens from TBLB. Immature fibroblastic foci and foamy alveolar macrophages are obstructing the alveolar ducts and adjacent alveoli. These features are consistent with BOOP.